USING PNA PROBES FOR HYBRIDIZATION-BASED ANALYSIS OF MIRNAS IN CAPILLARY ELECTROPHORESIS

MANSI ANAND

A THESIS SUBMITTED TO

THE FACULTY OF GRADUATE STUDIES

IN PARTIAL FULFILLMENT OF THE REQUIREMENTS

FOR THE DEGREE OF

MASTER OF CHEMISTRY

GRADUATE PROGRAM IN CHEMISTRY

YORK UNIVERSITY

TORONTO, ONTARIO

April 2019

ABSTRACT

MicroRNAs (miRNAs) are short non-coding RNA molecules (18–25 nucleotides) well-known for their post-transcriptional gene regulatory roles. The pathophysiology of various diseases (such as neurodegenerative, cardiovascular, *etc.*) and in particular cancer, have been characterised by the abnormal cellular expression levels of miRNAs. Therefore, validation and clinical implementation of reliable miRNA-based biomarkers would be appreciably helpful. To utilize miRNA potential in disease diagnosis and prognosis, accurate and robust quantitative approaches are required to analyze the sets of deregulated miRNAs (particular to a certain disease) in minimally-processed clinical samples. One such technique, developed by our lab, is direct quantitative analysis of multiple miRNA (DQAMmiR) using commercial capillary electrophoresis (CE) setting. The hybridization-based method is direct; does not require any miRNA processing or extraction, and just uses fluorescently labeled single stranded (ss) DNA probes and two kinds of mobility shifters: (i) single-stranded binding protein (SSB) in CE run buffer (binds to the excess probes and facilitate their separation from the hybrids), (ii) different length peptide drag tags conjugated to the ssDNA probes (render different charge: size ratios amongst the hybrids and enable their separation from each other); to simultaneously detect, separate and quantify multiple miRNAs. In my study, we introduced and developed a second-generation of DQAMmiR, which is simpler than the first-generation, as it omits the addition of SSB in CE run buffer by the use of uncharged Peptide Nucleic Acid (PNA) instead of ssDNA as the hybridization probes. The logistics behind incorporating PNA in our assay were derived based on the following considerations: PNA itself has no charge while the formed PNA–miRNA hybrids would possess partial negative charge (from miRNAs); this difference in charges should be sufficient to

resolve the excess of unbound PNA probes from the formed PNA–miRNA hybrids. Yet, the peptide drag tags would be required in order to separate the hybrids from each other. In proof-of-principle, the initial study was performed on a single miRNA to examine separation of the excess probe and formed hybrid. This was followed by the quantitative analysis of multiple miRNAs using complementary PNA/PNA-peptide probes. Overall, the assay proved to be accurate and precise for the analysis of three miRNAs, simultaneously. Ultimately, the performance of the assay was validated in presence of prostate cancer (PCa)-derived crude cell lysate for the analysis of two PCa-specific dysregulated miRNAs. The obtained results were found accurate, precise and robust, irrespective of sample matrix, even at low detection limits. With ongoing improvements, PNA-facilitated DQAMmiR is rapidly getting closer to its diagnostic applications in the clinical setups.

DEDICATION

Mother and Father: for believing in me and my potential

&

Maharaji: for being a constant support to boost my work

ACKNOWLEDGEMENT

I would like to thank all the people who contributed in some or the other way in the completion of my thesis. Foremost and most importantly, I would acknowledge Professor Sergey N. Krylov for accepting me in his lab. During my Masters tenure, not only he put in sheer efforts to channel my potential in the right direction, but also gave me intellectual freedom in my work, engaged me in new ideas, and demanded a high quality of work in all my endeavours. I also owe a token of thanks to Dr. Svetlana Krylova for her beneficial supervision and guidance for the completion of my project.

Every performed experiment and shown result was accomplished with help and support of fellow lab co-workers and collaborators. Liang Hu is the first in the list, I greatly benefited from his keen scientific insight, which also helped my work to improve for better (in my experiments, result analysis, manuscripts, reports, *etc*.). I also express gratitude to Victor for his technical expertise in my CE operations.

The rest Krylov group members of present and past, I am thankful to all for their warm presence and contributions during my stay in the lab. I gained a lot from this lab's vast chemistry knowledge and scientific curiosities.

Finally, I am grateful to Professor Derek Wilson and Professor Christopher Caputo for their time and insightful suggestions to further equip the project during the evaluations of my research work.

TABLE OF CONTENTS

LIST OF TABLES

LIST OF FIGURES

LIST OF ABBREVIATIONS

MiRNA/miR	MicroRNA
CE	Capillary Electrophoresis
LIF	Laser Induced Fluorescence
EOF	Electric Osmotic Flow
ss	Single-Stranded
μ_{EOF}	Electroosmotic Mobility for CE-running buffer
SSB	Single-Stranded Binding Protein
DQAMmiR	Direct Quantitative Analysis Of Multiple miRNA
PNA	Peptide Nucleic Acid
aa	Amino Acids
nt	Nucleotides
PCa	Prostate Cancer
LOD	Limit of Detection
LOQ	Limit of Quantification
CV	Coefficient of Variation
RSD	Relative Standard Deviation
ACN	Acetonitrile
LNA	Locked Nucleic Acid
q_H	Quantum yield of PNA probe relative to formed hybrid
q_P	Quantum yield of PNA probe relative to normalization probe
A	Peak Area
f/F	Function
$[P_0]$	Total probe concentration
S/N	Signal to Noise Ratio
SDS	Sodium Docyl Sulphate
mRNA	Messenger miRNA
UTR	Untranslated Region
RISC	RNA Induced Silencing Complex

Chapter One

INTRODUCTION

1.1 Biomarkers

The application of biomarkers in diagnosis and management of large number of diseases, such as cardiovascular disorders, infections, immunological and genetic disorders and, cancer in particular, is well-known [1]. Biomarkers can be defined as;

"a characteristic that is objectively measured and evaluated as an indicator of normal biological processes, pathogenic processes, or pharmacologic responses to a therapeutic intervention" - *National Institutes of Health Biomarkers Definition Working Group,* 1998

Diagnostic biomarkers are used to critically detect or confirm the presence of a disease or a condition of interest or to identify individuals with a subtype of the disease. The strengthening of the robustness of discovery technologies, particularly in genomics, proteomics and metabolomics, has been followed by intense discussions on establishing well-defined evaluation procedures for the identified biomarkers to ultimately allow their clinical validation and implementation. The importance of accurate diagnosis warrants the assessment of the clinical performance of diagnostic biomarkers [2]. The stages involved in biomarker development are shown in **Figure 1.**

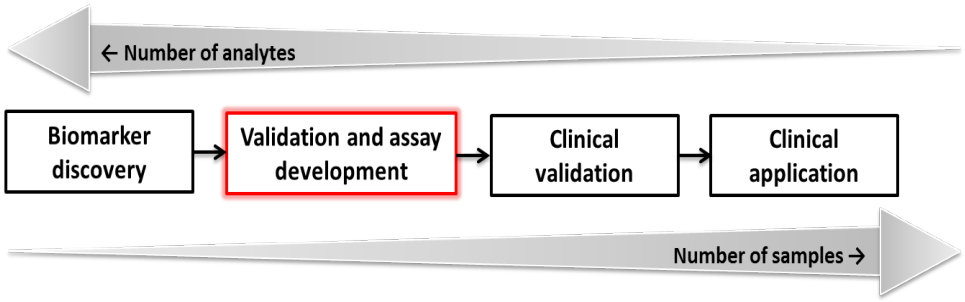

Figure 1: Stages in biomarker development involves multiple steps, linking initial discovery in basic studies, assay development and clinical validation and implementation. However, the validation and assay development (red box) is the rate-limiting step which is evident by low estimated rate (0.1%) of the successful clinical implementation of biomarkers [3].

The ideal diagnostic biomarker test should have 100% sensitivity (i.e., correct identification of the fraction of people with disease who test positive) and 100% specificity (i.e., correct identification of the fraction of people without the disease who test negative) [4]. However, the search of scientific literature clearly indicates that most of the published biomarkers are challenged either by the clinical sensitivity, specificity or more particularly, the robustness of the analytical techniques; therefore, inadequate to replace the existing clinical tests or only useful for detecting advanced disease stage, where the survival rate is low [5].

Nevertheless, in the view of urgent need for decent disease prognosis and treatment, which will positively impact the morbidity and mortality, the biomarker field is now moving more quickly towards clinical translation [6, 7] and significant research is now projected towards the identification of sound biomarkers, critical selection of analytical technique and development of the robust, accurate, sensitive, free of biases and cost-effective assays in practice.

1.2 Introduction to microRNA

The small non-coding RNAs families, such as 21–22 nucleotides short interfering RNAs (siRNAs), 26–30 nucleotides PIWI-associated RNA (piRNAs), 18–24 nucleotides microRNAs (miRNAs), and others; are well-known to perform multiple cell regulatory functions. However, miRNAs, in particular, is the most thoroughly investigated class due to their participation in up to 50% of the total gene regulatory events. MicroRNAs (miRNAs) function post transcriptionally by the interaction with 3-untranlated region (3'-UTR) of the coding mRNAs, to inhibit translation with or without degradation of the mRNA transcripts. They are evolutionary conserved and involved in the determination of cell fate and pattern formation in embryonic development and, control of cell proliferation, cell differentiation and cell death [8]. In addition, miRNAs have demonstrated a strong correlation with disease progression in cancer, cardiovascular disorders, neurodegeneration, and numerous other pathologies [9].

1.2.1 MiRNAs Biogenesis

Originally, discovered in *Caenorhabditis elegans* in the beginning of 1990s [10], the biogenesis of miRNAs takes place through multiple steps under tight temporal and spatial control (as shown in **Figure 2**). Following the transcription by RNA polymerase II, Drosha processes the primary miRNA transcript (pri-miRNA) into 60–100 nucleotides (nts) hairpin-like structure termed as the precursor-miRNA (pre-miRNA) in the nucleus. The formed pre-miRNA is transported out of the nucleus through the interaction with Exportin-5 and Ran-GTP. The exported pre-miRNA enters the cytoplasm, where it undergoes further processing ,catalysed by Dicer, to form 22-nts double-stranded (ds) RNA product containing both the mature miRNAs guide strand (miRNA) and the passenger (miRNA*) strand. These molecules are loaded by Dicer–TARBP2

complex into a large protein moiety, termed as RNA induced silencing complex (RISC) with specific regions for the hybridization to 3- UTR region in the target mRNAs. The silencing mechanism may be determined by the extent of base pairing between the miRNA and the target mRNAs (partial /complete), resulting in either translational suppression or degradation of the mRNA transcripts [11-13].

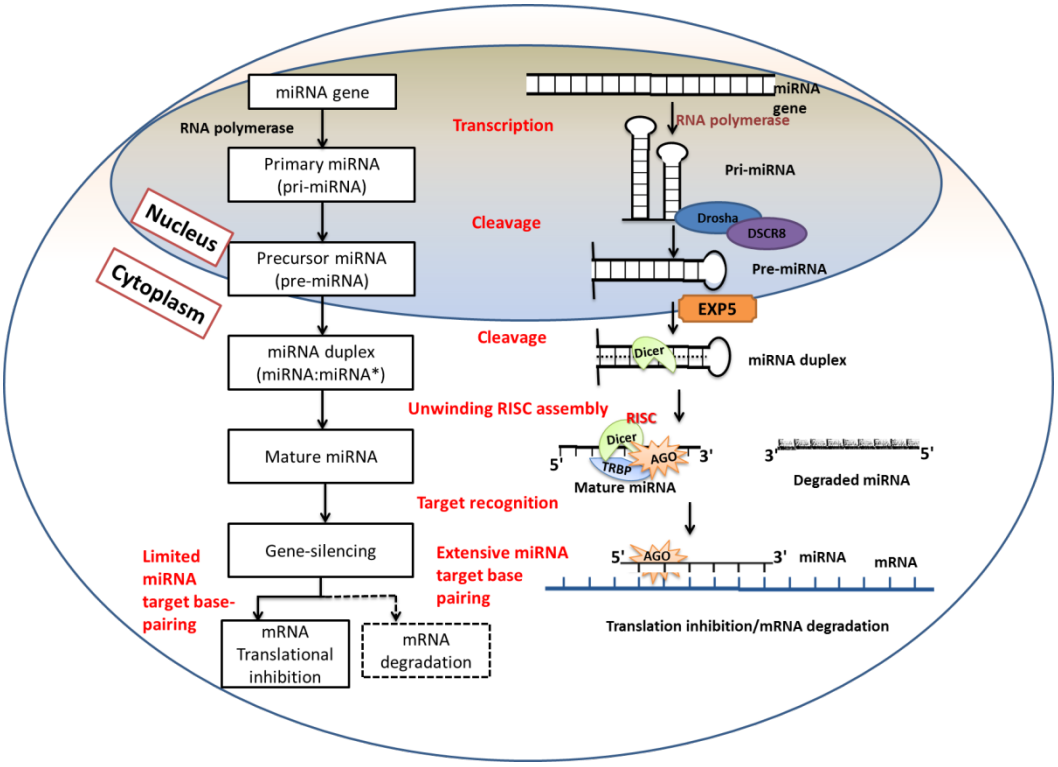

Figure 2: Biogenesis of miRNA. In nucleus, RNA polymerase transcribes the miRNA gene to produce a primary miRNA (pri-miRNA) molecule that undergoes nuclear cleavage (by Drosha and DSCR8) to form a precursor miRNA (pre-miRNA). The pre-miRNA is then exported (by Exportin-5 (EXP5)) to cyto-plasm, where in, it is cleaved (by dicer) to create miRNA:miRNA* duplex. Thereafter, the miRNA du-plex unwinds and the mature miRNA is assembled into RNA induced silencing complex (RISC). Based on the degree of complementary interaction between the mature miRNA and messenger RNA (mRNA), translation inhibition or degradation (less common) occurs.

1.2.2 MiRNAs Research Approaches

The wide involvement of miRNAs in gene expression has driven significant research efforts in the miRNA field. The current approaches focus mainly on determining: the presence and abundance of miRNAs, the specific targets of miRNAs and, their functional relevance in different biological context.

1.2.2.1 MiRNAs Detection. The identification and detection of regulatory miRNA is essential and foremost step in the miRNA research. The particular step is useful to determine whether or not miRNA is present and/or regulated in its abundance; and also, since the expression profile of the primary transcripts does not importantly corresponds to the mature miRNAs. There are various in-practices and -developing techniques to detect miRNA expression profile namely microarray, deep sequencing, real-time reverse transcription polymerase chain reaction, northern blotting, *in-situ* hybridization *etc* [14].

1.2.2.2 MiRNAs Target determination. The function of miRNA is ultimately defined by the genes it targets, and the consequential effects on their expression. The initial insight in miRNA`s targets can be obtained bioinformatically through a number of free available programs; such as miRBase and Targetscan. This is followed by more specific validation assays like Genome-wide target analysis, 3'UTR-reporter assays (provide functional evidence and even quantitate 3'UTR interaction effects in cell-based system) and pull-down assay (identifies the mRNAs that are bound to miRNA-processing proteins).

1.2.2.3 Regulation by miRNAs. The functional relevance of miRNAs is best studied by examining the phenotypic changes in culture or within an organism. There is now considerable work reported, both *in vivo* and *in vitro,* to study the regulation by miRNAs [15, 16].

1.2.3 MiRNAs as cancer biomarker in diagnosis

miRNAs regulate the expression of up to half of the human transcriptome and are well-studied for their functions in diverse regulatory processes including cell proliferation, cell death, fat metabolism, neuronal patterning, hematopoietic differentiation, immunity, *etc* [17]. Hence, in the diseased state, their altered expressions and differential enrichment is reflected in affected tissues and body fluids (plasma, serum, urine, *etc.*), respectively. In addition to differential expression profile, they are exceptionally stable in biofluids (including blood, urine, saliva, and others), as **Circulating miRNAs**, which allows relatively non-invasive sample collection and the collected samples are relatively easy to work within the laboratory settings [18-20]. With these useful biomarker characteristics, large research efforts have projected towards finding the sets of deregulated miRNA signatures (or miRNA fingerprints) that are representative of a specific disease. Specifically, a large sum of the total studies are designed to validate miRNAs for their use as cancer biomarkers [21]. MiRNAs appear to be located in genomic regions associated with cancer or at the sites coinciding with genes frequently rearranged or deleted. In these regions, they control important processes such as cell proliferation, apoptosis, and angiogenesis; dysregulation of which plays important role in the onset, progression, and metastasis of cancer [22, 23]. Numerous studies have shown distinct altered miRNA profiles in multiple cancer types, such as breast cancer, leukemia, liver cancer, ovarian cancer, pancreatic cancer, kidney cancer, prostate cancer and many more [24, 25]. Depending on the cellular context and the genes targeted, miRNAs can act as oncogene (promotes cancer progression) or tumor suppressor (suppresses cancer progression). Therefore, discovering miRNA expression patterns, unique to a particular cancer type, is an integral step in identifying biomarker signatures, potentially useful in its diagnosis [26].

1.2.4 Challenges in miRNA detection

There have been significant efforts invested over the past decade to develop or improve miRNAs detection methodologies. However, their detection is still challenging, owing to their unique characteristics, namely; short length (18–26 nts), low physiological abundance (hundred to few thousand copies per cell), large differences in melting temperature (due to heterogeneity in GC content), homologous sequences among the same family members, presence of the miRNA sequence in their biosynthetic precursor units (pre-miRNA), and discrepancies in number of expressed copies among different miRNAs. All these create problems in: labeling, selective amplification (introduces biases), simultaneous multiplexing studies, specificity and selectivity, and the detection of low expression miRNAs [27-39].

1.3 Detection of miRNAs

A wave of significant efforts is being made in combining the sets of such deregulated miRNAs into fingerprints (fewer than 10 miRNAs) to allow the discrimination between cancerous and non-cancerous cells [40, 41]. The identification of potential miRNA signatures can be performed on a relatively small number of samples by using microarray, a qualitative approach capable of simultaneously analyzing thousands of miRNAs. The validation of miRNA signatures, yet, requires more accurate quantitative analysis of relatively few miRNAs in thousands of samples. The analysis of thousands of samples can often be done by the cooperation of many laboratories; and essentially requires an analytical technology that is not only accurate, sensitive, target-specific, capable of detecting multiple miRNAs, but is also direct, fast, robust, and cost effective in practice [42-44]. Therefore, to better understand the work and development in the field

of miRNA analysis, it is important to critically evaluate the currently existing and emerging techniques for their clinical applications.

Classification

Undoubtedly, there has been a perennial work-flow to create new methodological platforms to satisfy the stringent requirements of miRNA validation assays. Yet, to better understand and in turn, evaluate their analytical power and clinical applicability, categorizing them, in principle, would be helpful. Notably, more or less all research approaches are integrated with one another to provide an efficient detection mode; however, they may be classified, if not strictly, based on their detection principle into following categories: spectroscopic, electrochemical and miscellaneous methods.

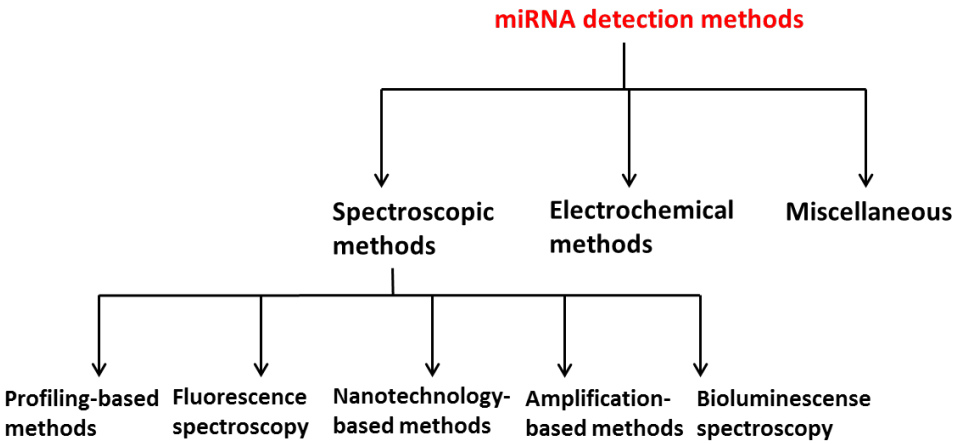

1.3.1 Spectroscopic methods

The analysis of miRNAs by these methods usually involves theoretical and experimental analysis of: fluorescent properties, single molecular approaches, electronic absorption and, electro-optical analysis of molecular interactions, structure and dynamics. The obtained spectra are

studied for the relative changes in intensity/shift in presence of miRNAs and, the obtained data is integrated and analysed.

1.3.1.1 Profiling-based methods

MicroRNA expression profiling is useful for miRNA identification and has been a field of interest for medicinal and biological research groups. **Northern blotting analysis** was previously the most standardized method for miRNA detection and still remains a gold standard for miRNA expression profiling, determination of their size and validation of predicted miRNAs (**Figure 3**) [44, 45]. However, there are some technical limitations that prevent its routine use including: low sensitivity, inability for multiple miRNAs detection, multiple handling steps and time-consuming procedures. Several labs had developed novel Northern blot version to improved sensitivity and reduce assay time, by either incorporation of Locked Nucleic Acid (LNA) or replacing conventional UV-cross-linking of RNA to chemically cross-linked nylon membrane [46, 47]. Recently, Bang and colleagues combined Northern blotting with laser ablation inductively couple mass spectrometry and employed lanthanide-labeled DNA probes for quantitative detection of multiple miRNAs [48]. Though the method offered improved sensitivity and specificity in simplex samples but the individual signals in the multiplex samples were indistinguishable, and moreover the assay was time-consuming; therefore is not practical in clinical studies, which require the detection of multiple and large numbers of RNA sample [14].

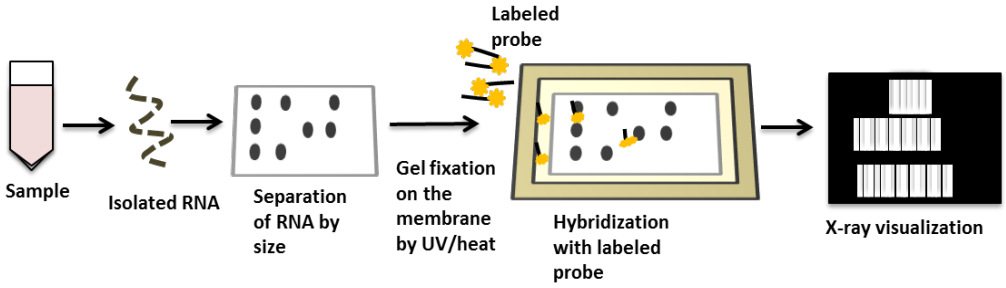

Figure 3: Schematic of Northern blotting

Currently, **microarray** represents the most widely used high-throughput method (**Figure 4**) for detecting the miRNA levels and particularly, to simultaneously screen large numbers of miRNAs signatures of various developmental stages and disease progression [49, 50]. However, the technique is challenged by several innate miRNA characteristics like short length (hampering both sensitivity and selectivity of the system), low abundance of certain miRNAs to total RNA content (<0.01%), and sequence homology among the family members. To overcome these challenges, in recent years, several nucleic acid analogues, like LNAs, are employed for their superior sensitivity [27, 51]. Reputed for miRNA identification, microarray lacks the ability to provide quantitative data, as the provided relative signal intensities do not rank the level of miRNAs abundance. Ultimately, large sample requirement and high expense in the fabrication of microarray chip limits its routine application in basic and clinical research laboratories [14].

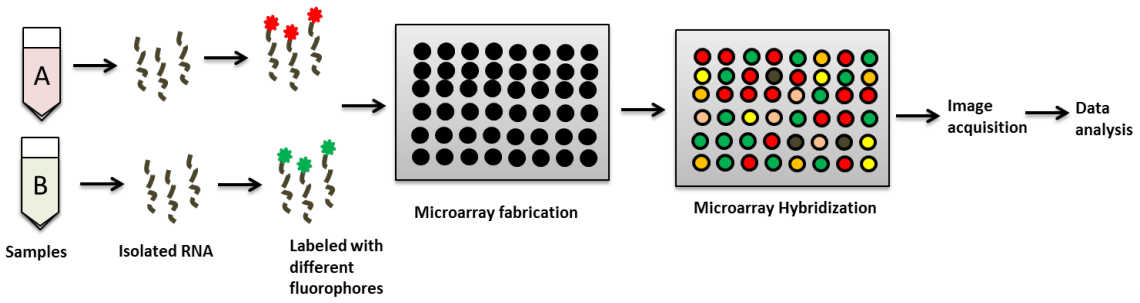

Figure 4: Schematic of Microarray

The other method known for its ability to monitor specific miRNA expression profiles and to provide spatiotemporally semi-quantitative data at the cellular and subcellular levels is **in-situ hybridization** (ISH). The technique is, however, impeded by low expression levels and reduced probe-binding affinity of miRNAs, due to their small size. Some innovations are put forward, either with the use of LNA probes, RAKE, hapten-like oligoes, tyramide signal amplification [52-57], to make ISH a robust and sensitive miRNA detection assay, but due to low quantification power and throughput, its use in diagnostics is limited [14].

1.3.1.2 Fluorescent correlation microscopy

The method uses microfluidic, multicolor laser system (capable of counting individual molecules) to distinguish among different molecules in solution, based on their unique spectral properties as they flow at high velocity through the system. Neely lab employed dual probe labeling system in conjugation with fluorescent correlation spectroscopy to count and quantify single molecules of miRNAs [58]. Li et al used Luminex **xMAP array**, a microsphere-based multiplex system capable of simultaneously detecting up to 100 analytes using one fluorescent reporter. Though straightforward, the method requires miRNA extraction and also, if the probes are not

sterically-bound (to quench the fluorescence of labeled probes in the absence of miRNAs) to the microspheres, they might result in increased background noise [59]. There are several other newly emerging methods for detection and quantification of miRNAs, such as; Lee and co-workers used graphically encoded **hydrogel microparticles** with fluorescent microscopy [60], the method is advantageous for its direct approach and sensitive detection, but require special and sophisticated instrumentation.

1.3.1.3 Nanotechnology-based methods

Several spectroscopic methods using nanotechnology have also developed in clinical science due to their exceptional photoelectric property, size and surface effects. For instance, label-free **Surface-enhanced Raman spectroscopy** for miRNA analysis. Though the method is rapid, it has certain shortcomings, such as, the spectra must be obtained individually prior to the assay (so as to identify the representative Raman shift) and also, sequences with overlapping peak cannot be differentiated, especially in presence of complex (biological) matrices. Zhou et al recently designed SERS sensor-based sandwich hybridization assay (as shown in **Figure 5**) for multiplexed miRNAs detection and quantification [61]. Despite the innovation being made, SERS technique requires sophisticated read-out system, specific analytical skills and convoluted data interpretations and verifications, rendering it rather impractical for molecular biology laboratories.

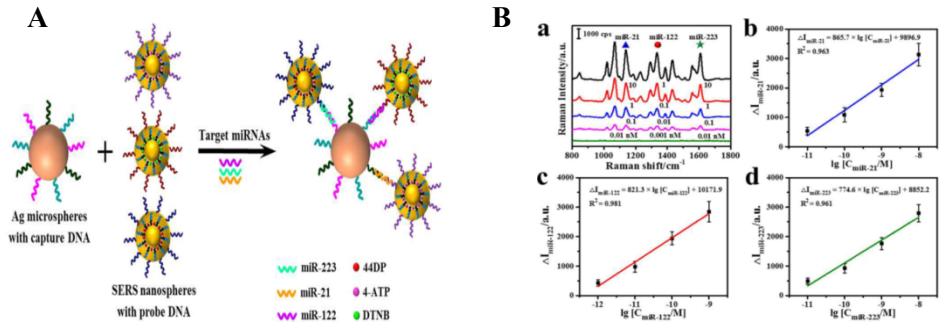

Figure 5: SERS-based sandwich hybridization assay: **A)** Schematic of the SERS-based sandwich hybridization assay which involves the reaction of SERS nanoprobes (with DNA probes complementary to miRNAs) and the Ag microspheres (with capture DNA, the miRNA first gets captured by Ag-HMS (silver hollow microspheres), followed by hybridization with SERS nanoprobes forming multiple sandwich hybridization complex. **B) (a)** Raman spectra obtained for simultaneous three miRNAs detection; **(b)(c),(d)** Standard curve between SERS intensities with log concentration of mir-21, miR-122 and miR-223, respectively. Adopted by Zhou et al [61].

Nanotechnology is also exploited for live cell miRNA imaging with regards to efficient loading and cellular delivery. Ryoo et al presented graphene oxide based miRNA sensor for quantitative monitoring of multiple miRNAs in living cells using dye-labeled PNA probes with low detection limit and high specificity [62]. Other work utilized amplification-based detection by the combination of gold-nanowires with quantum dots for miRNA live-cell imaging [63-65]. However, the need of special and costly equipment and background interferences of complex matrices, during analysis, makes them less robust.

1.3.1.4 Amplification-based methods

In the class of spectroscopic methods, to overcome the challenge of low physiological abundance of miRNAs, many lab groups have developed amplification-based assays to improve the sensitivity of the method by multifold. The quantitative **RT-PCR** (reverse transcription polymer-

ase chain reaction) is a well-known gold standard for miRNAs gene expression quantification (**Figure 6**). Several innovations, like extending the size of the mature miRNA by primer extension or using poly-A polymerase have also been reported [66, 67]. Unfortunately, these assays are costly for routine use in diagnostics, do not provide absolute quantification data and are prone to amplification-based biases.

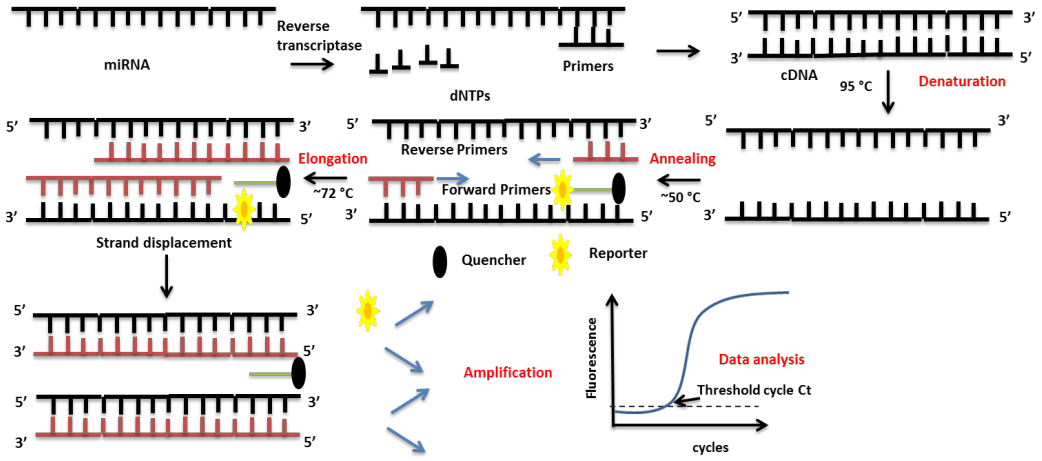

Figure 6: Schematic of RTqPCR using fluorescent quencher. The miRNA is firstly reverse transcribed to complementary DNA (cDNA), the formed cDNA undergoes the PCR cycle of denaturation, annealing (using forward and reverse primers) and elongation. During the elongation, the forward primer does the strand displacement reaction to release the reporter from quencher bonded probe to generate fluorescence.

The use of non-DNA polymerase enzymes (like endonuclease DNAase I) for amplified miRNA multiplexing studies using GO-protected polydopamine nanosphere DNA (multicolor sensor) fluorescent probes is also reported [68]. Despite an attractive approach, there are possibilities of high background noise and/or false signal due to failure in quenching. Several research groups have also performed **Ligase chain reaction (LCR)** [69, 70], **Rolling Circle Amplifica-**

tion (RCA) [71, 72] and one-step **exponential amplification reaction (EXPAR)** [73] for highly sensitive miRNAs detection. Another kind of enzyme-based amplification work is done using surface poly A-enzyme chemistry and gold nanoparticle-amplified SPRI measurements to detect multiple miRNAs at attomolar levels [74]. These methods have high quantitative power but the main technical limitations are: requirement of sophisticated and expensive instruments for signal readouts and, signal dependence on temperature.

To sum up, all the amplification–based methods have a long run-time to quantify miRNAs and may therefore delay prompt diagnosis. Additionally, they have disadvantages of high cost, lack of custom-made oligonucleotide probes, high levels of background fluorescence (due to in-complete fluorescence quenching), relatively poor reproducibility with increasing cycle number, and the most important, the need for amplification (risks of contamination and error during each amplification step); all these overweigh their potential clinical use [75, 76].

1.3.1.5 Bioluminescense spectroscopy

Bioluminescense detection methods have also developed for solid and in-solution miR-NA analysis by Cissell and offer advantages of minimal sample preparation, high throughput parallel analysis and high signal-to-noise ratio (**Figure 7**) [77, 78]. However, the method relies on decrease rather than increase in signal, which might pose a problem for detecting low abun-dance miRNAs.

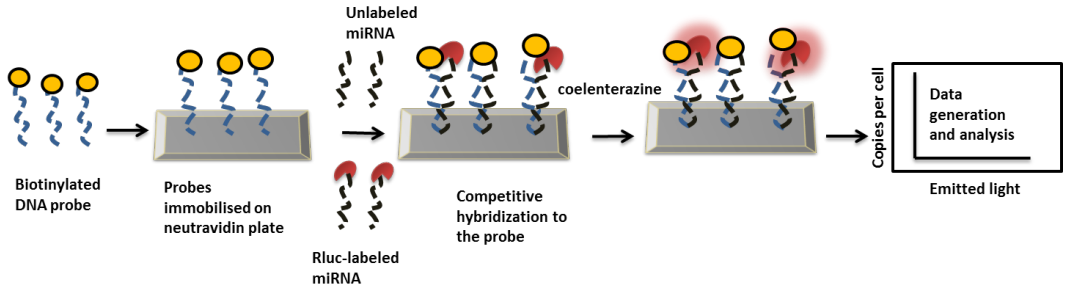

Figure7: Schematic of bioluminescence-based hybridization assay for miRNA detection which utilises protein complementation (reporter protein) of the luminescent enzyme Rluc.

1.3.2 Electrochemical detection methods

Electrochemical detection technology is among the emerging arena in terms of offering simple, efficient, and low-cost methods for quantitative miRNAs analysis. Monitoring the resistance of Peptide nucleic acid (PNA) functionalized silicon nanowires reported miRNA detection limit of 1 fM [79]. Another group used PNA capture probes immobilized onto a nanogapped biosensor array for miRNA analysis to provide a good dynamic range [80]. Gao and colleagues utilized direct chemical ligation to tag miRNAs, in a total RNA pool, with an electrocatalytic moiety [81, 82]. For quantitative multiplex detection, Berezoski et al designed 3-mode displacement-based electrochemical biosensing device [83]. The technique is highly sensitive and selective, yet being challenged by convoluted sample preparation which often introduces errors. Furthermore, the electrochemical detection instruments are usually not available in most laboratories which impede its widespread application in diagnosis.

1.3.3. Sequencing-based Methods

Next generation RNA sequencing has proved to be appreciably useful profiling technique to reveal the differential expression of miRNAs in several diseases and being capable in discriminating between homologous miRNA sequences [84, 85]. Extremely useful in the identification of miRNAs, their quantification abilities are still questionable.

1.3.3 Miscellaneous methods

These are other emerging methods in the field of miRNAs analysis. Lately, **biosensing devices** received considerable attention, example of which includes microfluidic devices and paper-based systems [86-90]. They are advantageous in terms of simplicity, sensitivity (in attomolar range), point of care and prompt miRNA analysis. However, they require miRNA extraction (variability in RNA yield), technical expertise and also their multiplexing abilities are doubtful.

Currently, **NanoString technology** has gained remarkable research panel interest of being a powerful identification and validation tool for miRNA biomarkers, by identifying their differential expressions in normal and cancerous state with appreciable sensitivity [91]. Though being direct and amplification-free; the method might not be sensitive for the detection of downregulated miRNAs; additionally, it is time-demanding (2 days) and requires very expensive consumables.

1.4 MiRNA analysis using Capillary Electrophoresis

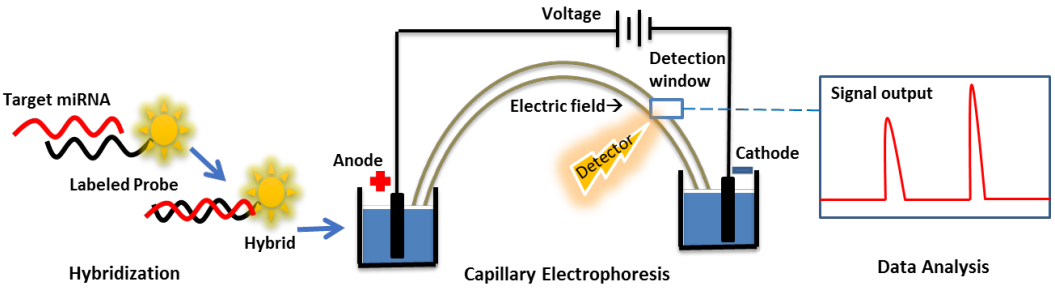

Figure 8: Schematic of Capillary Electrophoresis-based Hybridization assay

Capillary electrophoresis (CE)-based detection system (Figure 8) is another fast growing method for miRNA analysis. It is a useful analytical tool which offers advantages such as: high-throughput capability, good separation efficiency, rapid and cost-effective RNA and DNA analysis [92, 93]. In addition, the combination of CE with laser-induced fluorescence (CE-LIF) is one of the most sensitive detection modes in CE, providing great sensitivity and specificity for the analysis of trace biomolecules in complex sample matrices such as cell lysates, tissues, and various other biofluids [94, 95].

The use of CE for miRNA detection has been attempted since 2008, Li et al reported on miRNA and its methylated form (a crucial product in plant miRNA biogenesis), using capillary gel electrophoresis (CGE) and capillary zone electrophoresis (CZE) modes of separation [96]. Following, Chang et al CE-analyzed miRNA in nasopharyngeal carcinoma cell lysate without any non-specific interferences [97]. Since then, many researchers have presented various work related to miRNA detection using microchip or common CE systems [43, 98]. However, CE methods must overcome the problems, associated with separation efficiencies, sensitivity, speci-

ficity, and multiple target analysis, for them to be utilized in the screening and biological study of miRNAs in clinical samples. To address these, several appreciable works have been attempted to develop methods for the simultaneous, specific and sensitive detection of multiple disease-specific miRNA biomarkers in biological fluids. Above all, methods to improve the detection sensitivity of miRNAs in physiology are developing at faster pace.[99] Most of them are hybridization-based, principally involving the interaction between the miRNAs and their complementary labeled probes to form the respective hybrids/duplexes. Importantly, the hybridization efficiency is directly depended on the results obtained at specific hybridization conditions such as temperature, buffer components, and time. Therefore, determining the best hybridization conditions is necessary for the proper detection and analysis of trace amounts of miRNAs in complex biological samples [100].

Along with optimization of the hybridization conditions, the use of isotachophoresis (ITP) has been also reported to concentrate miRNAs in capillary columns by using CE or microchip CE systems. ITP is an electrokinetic focusing technique that utilizes a buffer system, composed of leading and tailing electrolytes with different conductivity or pH, to achieve sample preconcentration for more sensitive detection. Among these attempts, Schoch et al reported ITP technology for fast and ultrasensitive detection of small RNAs from total human RNA allowing the extraction, preconcentration, and quantification processes on the microchip CE system [98]. Garcia- Schwarz and Santiago achieved near 1 pM detection limit of miRNA in less than 10 min using ITP [101]. Further developments in CE detection systems and/or enrichment processes have also been continuously investigated to improve the assay sensitivity. The detection of multiple miRNAs in CE system is, usually, achieved using multiple detectors or probes. In addition, CE has been also combined with other assay methods to investigate the biological functions of

miRNAs, such as characterization of the miRNA binding site in miRNAs genes as well as quality control of extracted miRNA from biological samples [100, 102, 103]. Berezovski and coworkers developed a quantitative method for miRNA analysis in blood serum with protein-facilitated affinity CE with high sensitivity (300 molecules per microliter); they used single-stranded binding (SSB) protein (binds to fluorescently labeled DNA probe) and double stranded RNA binding protein (p19) (binds to DNA-miRNA Duplex) to facilitate separation. However, their method involved pre-concentration using PCR and also, scaling for multiple miRNAs analysis was questionable [104]. The same group further designed label-free and PCR-free protocol for direct detection of cancer- related endogenous miRNAs combining CE with electrospray ionization-mass spectrometry. Though method is direct, however, its quantification power is low [105]. Sets of miRNAs are also been used for performing body fluid identification using CE and proven to have similar discriminatory power as qPCR [106].

Though appreciable work using CE-based hybridization assay has been reported in the field of detection and quantitative analysis of miRNAs, but the use of excess of complementary probes (which render similar electrophoretic mobilities as to formed miRNA-probe hybrids) poses separation difficulties and therefore, affects the accuracy of miRNA quantification. In addition, in the light of multiplexing studies, miRNAs being nearly similar in terms of charge and size, their separation from each other in CE is another bottle-neck needed to address for the clinical application of CE-based miRNA hybridization assays. Nonetheless, with sound knowledge of the limiting factors and their underlying mechanisms, researchers have come up with approaches to overcome them. Our lab, also put in intense efforts in this arena and presented an amplification-free direct quantitative analysis of multiple miRNA (DQAMmiR) using CE-based

hybridization more than a decade ago and since then, have continuously worked to improve it even further.

1.5 Direct Quantitative analysis of multiple miRNAs (DQAMmiR)

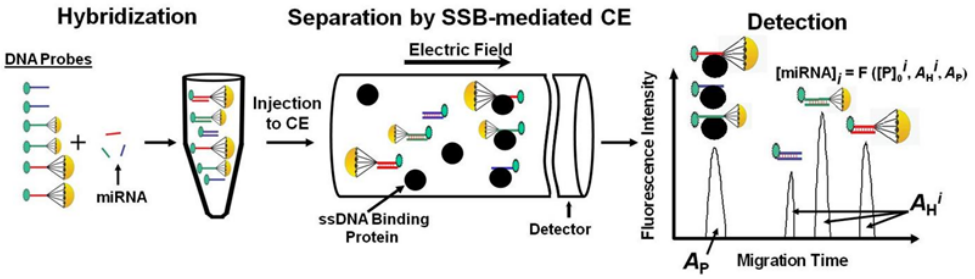

Figure 9: Schematic of direct quantitative analysis of multiple miRNAs. The CE-based hybridization-assay involving the hybridization of miRNAs with their complementary probes (with/without drag tags) and taking the advantage of separation abilities of CE to resolve the hybrids and excess unbound probes for the accurate quantification of miRNAs using mathematically derived equations.

The direct quantitative analysis of multiple miRNAs (DQAMmiR) **Figure 9,** worked and developed by our lab, is the first direct assay that did not require any target modifications and provided absolute miRNAs quantitative data. Briefly, it is a hybridization assay which utilises the separation abilities of capillary electrophoresis to analyse multiple miRNAs. To address the (earlier mentioned) separation inefficiencies, two following approaches were used: 1) the addition of single-stranded binding protein (SSB) in the CE running buffer to separate hybrids from excess unbound probe and, 2) the conjugation of peptide drag tags on the complementary oligonucleotide probes to separate the hybrids from each other during multiple miRNAs analysis. Since the method inception, efforts were made to improve the multiplexing abilities, limit of de-

tection and specificity. For simultaneous detection of five miRNAs, different length peptide tags (acted as mobility shifters) were conjugated to the respective DNA/LNA probes in order to resolve the similar mobility hybrids from each other. Furthermore, to reduce the overall assay time by the use of large probe concentration relative to target, a purification procedure was used to significantly reduce the probe impurities and accelerate the hybridization kinetics. Combining DQAMmiR with capillary isotachophoresis, (in-capillary pre-concentration technique) was another benevolent innovation that improved the limit of detection by two orders of magnitude, scaling our assay to low abundance miRNAs. The assay by this stage was highly sensitive and accurate in analysis, however, sequence homology of different miRNAs posed the specificity problem, which our group solved by: 1) introducing LNA bases to DNA oligonucleotide probes, which improved the specificity by increasing the *Tm* (melting temperature) of the hybrids and, 2) running CE under dual-temperature mode, i.e., high capillary temperature at the beginning for specific hybridization, followed by low capillary temperature for the following CE run, to avoid any adverse effects on electrophoretic separation of the hybrids. With this, the assay was specific to even a single nucleotide mismatch and added to the overall benefits of the DQAMmiR.

Yet, despite of being a well-developed approach, the assay lacks the robustness for working at different CE temperatures; in terms of introduction of a protein (SSB) for the separation of target-bound probes from target-unbound probes. SSB being a protein is quite thermolabile and also might have some quenching phenomena on the fluorescently labeled probes which could overall decrease the assay potential along with increasing the cost, making it less likely suitable for clinical setups [40, 42, 107-113].

Chapter Two

PEPTIDE NUCLEIC ACID (PNA)-FACILITATED DQAMIR

The presented material was published previously and reprinted with permission from *Hu, L.; Anand, M.; Krylova, S.M.; Yang, B.B.; Liu, S.K.; Yousef, G.M.; Krylov, S.N.* ***Direct quantitative analysis of multiple microRNAs (DQAMmiR) with peptide nucleic acid hybridization probes.*** *Analytical Chemistry 2018, 90, 14610–14615.*

Here we introduce the second-generation DQAMmiR, which is simpler than the first-generation assay, as it does not need Single Stranded Binding protein (SSB) and requires only peptide drag tags on the probes to carry out the simultaneous quantitative analysis of multiple miRNAs. The reason for using SSB in the first-generation DQAMmiR was to separate the excess unbound ssDNA probes from the ssDNA-miRNA hybrids. The probes and hybrids, otherwise, cannot be resolved due to their similar electrophoretic mobilities with regards to similar charge to size ratio (negative charges on both DNA and miRNA strands). SSB would not be needed if the probes are polymers capable of hybridizing miRNA but are not negatively-charged. An example of such polymers is peptide nucleic acid (PNA), an electrically neutral analogue of DNA [114].

2.1 Introduction to PNA

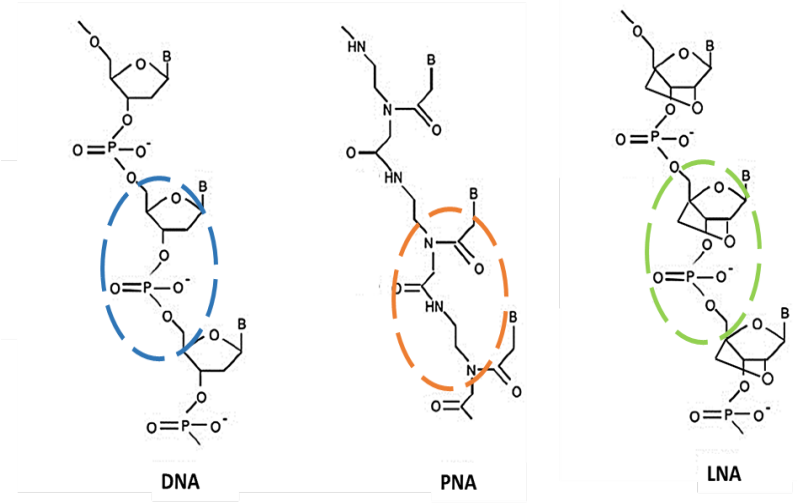

Figure 10: Structural comparison between different probes employed in hybridization assays; DNA, PNA (Peptide Nucleic Acid) and LNA (Locked Nucleic Acid) probes. There is difference in the backbone among the three probes: Blue: negatively charged ribose phosphate units in DNA, Orange: uncharged N-aminoethyl glycine units in PNA, and Green: O-linker between C1 and C4 in negatively charged ribose phosphate units in LNA.

PNAs (**Figure 10**), are engineered uncharged oligonucleotide analogues, first synthesized by Nielson et al (1991) [115], in which, the neutral polyamide scaffolds (N-(-2-aminoethyl glycine units) replaces the usual negatively charged phosphodiester backbone, yet homomorphous to DNA, with respect to the number of backbone bonds and the distance between the backbone and the nucleobases. PNA oligomers are solid phase-synthesized using Bhoc (benzhydryloxycarbonyl) or Fmoc (9-fluorenylmethoxycarbonyl chloride) chemistry. Nielson and group used Bhoc chemistry with an automated peptide synthesizer.[116] However, the particular involves the repetitive use of extremely hazardous trifluoroacetic acid. On the other hand, Fmoc uses much milder reaction conditions and can also be used with DNA synthesizer (unlike Boc);

nonetheless, it produces PNA oligomer with more impurities, some generated by trans-acylation reaction which are difficult to separate because of identical molecular weight and similar properties [117]. Recently Bts chemistry, developed by Panagene, uses self-activated building blocks which produce more pure form of PNAs. Importantly, it does not add building blocks to a misbehaved product and hence, the impurities are of smaller molecular weight and can be easily removed by HPLC purification [118].

PNAs offer stronger hybridization behavior to complementary DNA, RNA or PNA itself and the formed duplexes have high thermal stability and unique ionic strength effects [119]. The distinct physio-chemical properties of PNAs, such as great biological stability (resistant to nucleases, proteases, *etc.*), appreciable chemical simplicity, excellent nucleic acids binding properties (lack of repulsion in reaction due to its uncharged backbone) even at low ionic strength conditions (which discourages the annealing of complementary genomic strands) [120], and much of our interest, the uncharged electric behavior, compared to partial negative nature of potential PNA–miRNA hybrids, make them the probe of choice for DQAMmiR.

There are quite a few previous reports of using PNA in CE-based hybridization assay for the analysis of small ss-oligos, the earliest work on PNA was presented by Perry et al in CE-LIF showing decent separation between the formed PNA–ssDNA hybrid and the excess unbound-PNA, reflecting the mobility difference between the two under the applied electric filed; additionally, the lab also reported PNA`s ability to detect single and double nucleotides polymorphism in presence of a denaturant [120]. Following this, the other group also validated the specificity of PNA probes to single nucleotide polymorphism (SNP) in CE-LIF probe assay for single-base pair mutated DNA [121]. The experimental results showed PNAs as less tolerant to mismatches (the formed mismatch hybrid are unstable due to reduced *Tm* (loss of 8–25 °C)). In

addition, there are some reported qualitative and quantitative binding studies of PNA to target ssDNA/ RNA in multiple CE modes, showing the stability and comparatively more favorable binding properties [122]. Alternatively, Ostromohov group presented ITP-based amplification-free assay using PNA for rapid and highly sensitive (LOD~100fM) detection of short-chain nucleic acids with improved S/N ratio [123]. The peptide backbone in PNA is readily available for chemical modifications like attaching peptide chain, PEG polymers, *etc*; to enhance its nucleic acid binding or convey other desired properties to the molecule [92, 93, 124].

The use of PNA in the field of miRNA analysis has since been confirmed by a group who utilised PNA in the form of 'fluorogenic biosensors' to target miRNAs specific to prostate cancer [125]. A quantitative and multiplexed miRNA sensing system (PANGO) in living cells was designed by Ryoo et al which showed detection limit as low as ~ 1 pM [62]. The other useful applications of this uncharged synthetic oligonucleotide include; PNA-microarray for miRNA expression profiling and also, *in-vitro* studies indicate their use in antigene, antimiR and antisense therapies [126].

2.2 Justification for the use of PNA in DQAMmiR

As noted, the physiochemical properties of PNA and previously performed work quite clearly justify its potential use to solve the inherent separation inefficiencies encountered in CE-based probe assay. PNA-facilitated DQAMmiR involves the hybridization of fluorescently-labeled PNA probes to the complementary negatively charged miRNAs to form stable duplexes (PNA–miRNAs) in solution, followed by detection, separation and quantification of excess probes and hybrids in CE-LIF mode (which separates molecules based on the difference in

charge : size ratio). An improved separation between the hybrids and excess PNA probes is expected, likely omitting the need of an external mobility shifter (such as SSB). However, PNA have certain limitations in use; unlike, usual charged oligonucleotide probes, the hydrophobicity of PNA promotes self-aggregation and nonspecific adherence, posing technical challenge for its handling in solution, and particularly in our assay, the probability of sticking to the capillary walls (severely affecting miRNA quantitative accuracy) [127]. To combat the solubility issues, some structural modifications to PNA have been reported: addition of amino acid residues at their termini [128], conjugation to charged DNA molecules,[129] or to high molecular weight polymers like PEG [130]. We, in our assay, employed PNA probes attached to adjacent O-linkers/AEEA (2-aminoethoxy-2-ethoxy acetic acid) which acts as solubility enhancer and also added 20% acetonitrile (ACN) to the CE running buffer. Not only ACN aids the delivery of PNA into the solution but also prevents PNA sticking, by forming a hydrophobic layer on the capillary walls. In addition, since the viscosity of ACN is less than water-based solution, therefore, the effect of 20% ACN tends not to adversely affect Electroosmotic flow (EOF) in CE, which was further justified by theoretical calculations of viscosity and obtained experimental results [131].

However PNAs, being uncharged pseudo-oligonucleotides have physiochemical properties significantly different from commonly employed polyanionic oligonucleotides, therefore, any experimental conditions optimized for hybridization or CE analysis for usual oligonucleotides cannot be concluded as optimal for PNA. Nonetheless, to achieve the absolute quantification of multiple miRNAs simultaneously, a decent separation of individual PNA–miRNA hybrids from each other is the most needed. Hence, peptide drag tags will be attached to PNA probes (similar to first generation DQAMmiR) to alter the mobility of the hybrids. All things be-

ing considered, we planned our experimental layout as follows; 1) Analysis of a single miRNA, 2) Analysis of multiple miRNAs.

2.3 Analysis of a single miRNA

The initial method development for efficient hybridization and CE separation was achieved by performing a single miRNA analysis. The prime goal for this study was to achieve the separation of target-bound and target-unbound excess probe. For this, a single miRNA was selected (*hsa-miR-21*) and the conditions for hybridization (target and probe concentrations, temperature, buffer components, incubation time, *etc.*) and CE-LIF detection were determined. For quantitative purpose, we incubated different miRNA concentrations (500 pM–31.25 pM) with constant 10 nM PNA probe in triplicates and the obtained CE-data was precisely quantified.

2.3.1 Method and Materials

2.3.1.1 MiRNA and complementary PNA probe. The miRNA (5'-UAG-CUU-AUC-AGA-CUG-AUG-UUG-A-3') was custom-synthesized by IDT (Coralville, IA, USA) and the fluorescently-labeled PNA probe (Alexa 448-O-5'-TCA-ACA-TCA-GTC-TGA-TAA-GCT-A-3') was custom-synthesised by PNA Bio, Inc. (Newbury Park, CA).The other chemicals were obtained from Sigma-Aldrich (Oakville, ON, Canada) unless stated otherwise.

2.3.1.2 Hybridization Conditions. The hybridization reaction was performed in Mastercycler 5332 thermocycler (Eppendorf, Hamburg, Germany). Various concentrations of miRNA were incubated with 10 nM PNA probe in CE-running buffer. The temperature was increased to a denaturing 95 °C and then lowered to 60 °C at the rate of 20 °C/minute and was held to 60°C for

30 min to allow annealing. In order to minimize miRNA degradation, a nuclease-free environment was maintained.

2.3.1.3 CE-LIF. All experiments were performed using a P/ACE MDQ CE instrument (Beckman-Coulter, Fullerton, CA, USA) equipped with a LIF detector. A 488 nM line of continuous wave solid-state laser (JDSU, Santa Rosa, CA, USA), with 1 mW effective output was utilized to excite fluorescently labeled probes. Fluorescence signal was detected at 520 nM wavelength. A bare fused-silica capillary with an outer diameter of 365 μm, an inner diameter of 50 μm, and a total length of 80 cm was used. The distance from the injection end of the capillary to the detector was 70 cm. Prior to each run, the capillary was flushed with 0.1M HCl, 0.1 M NaOH, deionized H_2O, and the running buffer (20 mM borax 20% (v/v) acetonitrile pH 9.0) for 2 minutes each. Samples were injected at the positive end by a pressure pulse of 0.5 psi for 5seconds; the volume of the injected sample was ~ 6 nL. Electrophoresis was driven by electric field of 312.5 V/cm applied voltage and at coolant controlled temperature 20 °C. The electropherograms were analysed using 32 Karat software. Peak areas were divided by the corresponding migration time to compensate for the dependence of the residence time in the detector in the electrophoretic velocity of analyte.

2.3.1.4 Spectrophotometric Determination of Target and Probe Concentrations. The target and probe concentrations were determined by light absorption at 260 nm using the Nano-Drop ND-1000 spectrophotometer (Thermo-Fisher Scientific). The stock concentration of the target and probe was too high to measure directly; therefore, a small sample of the each stock solution was serially diluted, and absorbance of each sample at 260 nm was measured 5 times. The concentration of each sample was determined as $\boldsymbol{absorbance/\varepsilon l}$ where ε is the molar extinction coefficient of the miRNA-21 and PNA probe at 260 nm respectively (provided by IDT/PNA Bio) and

l is the optical path length. Using the concentrations of the serial dilutions, the original stock concentration was extrapolated.

2.3.2 Result and Discussion

2.3.2.1 Separation between the excess probe and PNA–miRNA hybrid in CE. The separation between excess probe and formed hybrid is the foremost requirement to accurately quantify the miRNA concentration and indeed to justify the use of PNA in DQAMmiR. For the given experiment, 1 nM miRNA-21 was allowed to hybridize with 10 times higher PNA probe concentration (10 nM), followed by CE-LIF detection. The obtained electropherogram showed an excellent separation between excess probe and formed hybrid (**Figure 11A**).

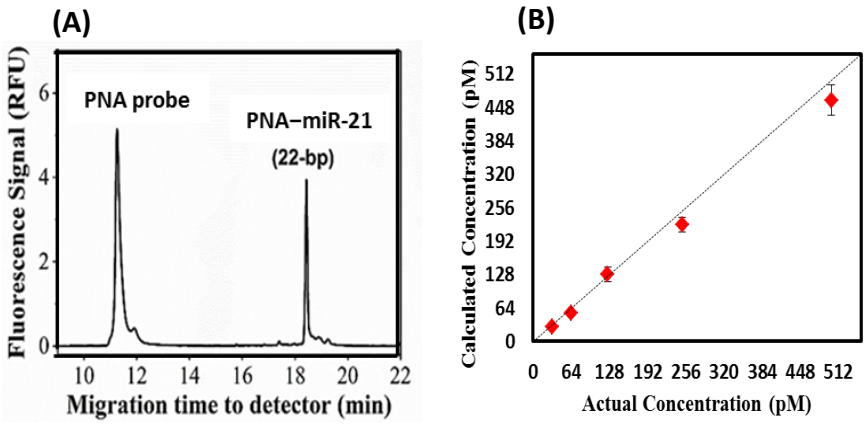

Figure 11: A) CE separation of a PNA probe from a PNA–miR-21 hybrid in a run buffer of 20 mM borax 20% (v/v) acetonitrile pH 9.0. The sample was prepared by incubating 1 nM of miR-21 with 10 nM PNA probe. Separation was driven by an electric field of 312.5 V/cm at 20 °C. **B)** Quantitative plot between PNA-facilitated DQAMmiR measured concentrations and spectroscopically determined concentrations (31.25 pM–500 pM) at 260 nm for miR-21. The dashed line (y = x) represents a line corresponding to 100% recovery. Error bars represent standard deviations from mean values obtained from three experiments.

2.3.2.2 Quantitative analysis of miRNA

2.3.2.2.1 Determination of Quantum Yield (q_H). Assuming that the probe can be baseline separated from the hybrid, the quantum yields of the target-bound probe, q can be found from two sets of data obtained for the same amount of the probe with and without the target, respectively:

$$q_H = \frac{A_H}{A_{P_0} - A_P}$$

Here, A_{P_0} is the fluorescent signal of the probe for no target and A_P and A_H are fluorescent signals of the remaining target-unbound probe and target-bound probe, respectively, for a nonzero target concentration.

2.3.2.2.2 Determination of miRNA concentration. Theoretical Consideration; we assume that the labeled PNA probe hybridizes with the miRNA in a process that goes to completion:

$$\text{PNA} + \text{miRNA} \rightarrow \text{PNA–miRNA} \quad (1)$$

The probe is taken in excess to the miRNA. In equilibrium, the initial amounts of the probe and target, P_0 and miRNA, are linked with the amounts of the remaining probe, P and formed hybrid, PNA–miRNA, as:

$$[P_0] = [\text{PNA–miRNA}] + [P] \quad (2)$$

For $[P_0] \gg [\text{miRNA}]$ & $[P_0] \gg K_d$, hence;

$$[\text{PNA–miRNA}] = [P_0] - [P] \quad (3)$$

In the equation (3), the amounts could be expressed in any conventional units such as moles or number of molecules. In the following work, symbols A with corresponding indexes

denoted measurable areas of peaks in electropherograms, equivalent to integrated fluorescent signals and was presented in arbitrary units. To compensate for differences in the residence time in the detector, the areas were divided by corresponding migration times. The quenching effects of the target annealing were also taken into account by the introduction of q_H as the relative quantum yield of the target-bound probe with respect to that of the unbound probe.

$$[\mathrm{P}] = aA_P \tag{4}$$

$$[\mathrm{miRNA}] = a\left(\frac{A_H}{q_H}\right)_P \tag{5}$$

Using equation (4) and (5) in equation (3);

$$a\left(\frac{A_H}{q_H}\right) = [\mathrm{P}_0] - aA_P$$

We could express the initial total amount of the probe as;

$$[\mathrm{P}_0] = a\left(\frac{A_H}{q_H} - A_P\right) \tag{6}$$

Hence,

$$a = \frac{[\mathrm{P}_0]}{\frac{A_H}{q_H} - q_H} \tag{7}$$

The final amount the miRNA could be found by substituting the coefficient a from equation (7). On simplification the final equation was obtained as follows;

$$[\text{miRNA}] = \frac{[P_0]}{\frac{A_H}{q_H} - A_{P_0}} \cdot \frac{A_H}{q_H}$$

$$[\text{miRNA}] = \frac{[P_0]}{1 + q_H\left(\frac{A_P}{A_H}\right)} \tag{8}$$

Hence, the target concentration was a function of initial concentration of the probe, area of the target-unbound and target-bound probe, and the quantum yield;

$$[\text{miRNA}] \rightarrow f([P_0], A_P, A_H, q_H)$$

In above expression, $[P_0]$ is known; q_H could be determined prior to the sample analysis; A_H , A_P, A_{P_0} could be measured by CE run directly.

2.3.2.2.3 5-point Quantification for a Single miRNA. The quantitative analysis was performed for different concentration of miRNA (500, 250, 125, 63.5, and 31.25 pM) incubated with a constant PNA probe concentration (10 nM), followed by CE analysis. The CE results were quantified (**Table 1**) and the measured concentrations were plotted against the spectroscopically determined concentrations (**Figure 11B**). A recovery between 90–113% and RSD <15% indicated the accuracy of the assay.

Table 1: Quantification results and recovery (%) obtained from PNA-facilitated DQAMmiR for a single miRNA analysis corresponding to the actual concentrations as determined by spectroscopically at 260 nm. Standard deviations from mean values were obtained from three experiments.

Actual concentration (pM)	PNA-faciliated DQAMmiR concentration (pM, Mean ± Standard Deviation)	Recovery (%)
500	502 ± 11	100
250	249 ± 5	99.6
125	135 ± 6	108
62.5	71 ± 8	113
31.25	33 ± 2	105

2.3.3 Conclusion

The basic goal to carry a single miRNA analysis was to check the feasibility of PNA probe in DQAMmiR, but more particularly to achieve decent separation between the excess of PNA probe (uncharged) and formed PNA–miRNA (partially negatively charged) in CE. The preliminary data well-established the use of PNA in omitting SSB (as mobility modifier for unbound probes) in DQAMmiR.

2.4 Multiple miRNA Analysis

Often, different miRNAs collectively regulate important cell regulatory events and, thus can be simultaneously involved in the progression and development of diseases. Therefore, it becomes useful and often necessary to monitor multiple miRNAs at the same time to better understand the diseased state. The detection of multiple miRNAs is also useful for the discovery of new biomarkers and/or to monitor multiple biomarkers for the improvement of specificity and sensitivity of diagnostic tests.

2.4.1 Theoretical estimation of PNA–miRNA hybrids mobility

PNAs possess negligible charge; yet the size of PNAs differ only slightly from usual oligo (ssDNA, RNA) in terms of rise in the length per base pair addition; possibility due to the difference in the backbone units (N-aminoethyl glycine instead of ribose phosphate units). Keeping this in mind, (as earlier being designed for DNA–miRNA hybrids), a theoretical model for PNA–miRNA hybrids was evolved, by Liang Hu, Ph.D candidate in our lab, to predict their electrophoretic mobilities in CE, with strict consideration of probable variations for PNA probes in relation to usual DNA probes. Similar to DNA–miRNA, PNA–miRNA hybrid was assumed to be a rigid rod, as for short nucleobase hybrids [132];

$$L_{\text{hyb}} << b_{\text{K}}$$

Here, L_{hyb} is the contour length and is equal to $N_{\text{hyb}} \cdot b$, in the range of 4–6 nm for possible PNA–miRNA hybrids (N_{hyb} is the number of base pairs, 18–25 nts for miRNAs; and b is the helical rise per nucleobase, 0.24 nm for PNA–RNA hybrid [133], and b_{K} is the Kuhn length which is though not yet reported for PNA–RNA hybrids, but the latter has proven to be stiffer as compared to dsDNA (for which b_{K} is in the range of 30–50 nm) [134]. Hence, PNA–miRNA hybrid was assumed to be a stiff rod moving along the capillary axis under applied voltage. Taking the model as the lead, the CE-mobilities for possible PNA–miRNA hybrids were estimated. Following the expression of two forces, i.e. electric force ($F_{\text{E,hyb}}$) and hydrodynamic frictional ($F_{\text{f,hyb}}$) force, acting on species [135, 136]:

$$F_{\text{E,hyb}} = \frac{eL_{\text{hyb}}}{z_i \lambda_{\text{B}}} E \tag{9}$$

$$F_{\text{f,hyb}} = 2\pi\eta L_{\text{hyb}} u_{\text{rel}} \left(\ln \frac{2L_{\text{hyb}}}{d_{\text{hyb}}} - 0.72 \right)^{-1} \tag{10}$$

Here, E is the applied electric field, z_i is from the literature, d_{hyb} is the diameter for PNA–RNA hybrid, calculated as 3.5 nm [133]. The viscosity, η for 20 % acetonitrile buffer solution was comprehended from the earlier reports as 1.1 mPa.s [137] and the Bjerrum length was calculated as 0.79 nm using;

$$\lambda_B = \frac{e^2}{4\pi\varepsilon_0\varepsilon_r k_B T} \tag{11}$$

In equation (11), elementary charge, e is 1.602×10^{-19} C; vacuum permittivity, ε_0 is 8.85×10^{-12}; relative dielectric constant, ε_r is ~72 [136], Boltzmann constant, k_B is 1.38×10^{-23} at absolute temperature, u_{rel} is the velocity of the hybrid in the running buffer. Hence, the mobility of the PNA–miRNA hybrid could be estimated by balancing the electric and hydrodynamic forces

$$F_{E,hyb} = F_{f,hyb} \tag{12}$$

From equation (9), (10), and (12),

$$u_{rel} = \frac{e}{2\pi z_i \eta \lambda_B}\left(\ln\frac{2N_{hyb}b}{d_{hyb}} - 0.72\right)E \tag{13}$$

Since, $\mu_{hyb} = \frac{u_{rel}}{E}$, where μ_{hyb} is the electrophoretic mobility of the hybrid; therefore, equation (13) could be expressed as;

$$\mu_{hyb} = \frac{u_{rel}}{E} = \frac{e}{2\pi z_i \eta \lambda_B}\left(\ln\frac{2N_{hyb}b}{d_{hyb}} - 0.72\right) \tag{14}$$

According to the equation (14), it could be derived that the electrophoretic mobility of the hybrid was dependent on the number of nucleotides present in the miRNA. To confirm the accuracy of the model, a preliminary work was performed for miRNA-21 (N_{hyb} = 22-nts) to verify, if the theoretical mobility estimations of PNA–miRNA hybrid does corresponds to the experimentally obtained results. The theoretically estimated and experimentally calculated mobility of PNA–miRNA-21 were found to be 1.12×10^{-4} $cm^2 \cdot V^{-1} \cdot s^{-1}$ and 1.20×10^{-4} $cm^2 \cdot V^{-1} \cdot s^{-1}$, respectively. The error between the particulars was within the acceptable limits, which suggested that our model was appropriate to our study design. The electroosmotic mobility(μ_{EOF}) for the CE running buffer (20 mM borax 20% (v/v) acetonitrile pH 9.0) was calculated experimentally as 3.14×10^{-4} $cm^2 \cdot V^{-1} \cdot s^{-1}$ at 20 °C.

The simulated electropherograms (**Figure 12**) for PNA–miRNA hybrids differing in number of nucleotides of miRNAs was derived using Gaussian function by plotting *f(t)* corresponding (t_0, σ);

$$f(t) = e^{-\frac{(t-t_0)^2}{2\sigma^2}} \quad (15)$$

Here, t_0 is the theoretically estimated migration time, σ is the peak variance correlated to the peak width and was obtained by fitting the experimental results with the Gaussian function for peak of unbound PNA probe and PNA–miRNA hybrid, respectively. The velocity and the migration time were calculated using the given constant parameters: L_{cap}, length of the capillary as 80 cm; L_{det}, effective length (distance between inlet and detector) as 70 cm and E, electric field strength as 312.5 V/cm.

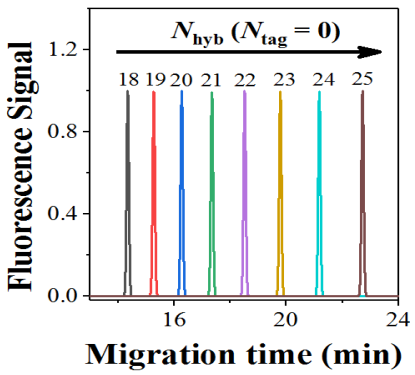

Figure 12: Simulated electropherogram of PNA–miRNA hybrids differing in number of nucleotides among the miRNAs (18–25 nts.). Migration times of peaks shown above were estimated by using $\mu_{EOF} = 3.14 \times 10^{-4}$ $cm^2 \cdot V^{-1} \cdot s^{-1}$ which was experimentally measured for CE-run buffer containing 20 mM borax 20% (v/v) acetonitrile at pH 9.0.

2.4.2 Universal Peptide drag tags for separation of similar length targets

The theoretical model concludes, given that, if the number of nucleotides differs among the miRNAs by at the least single-base pair, the individual PNA–miRNAs could be separated without the need of any modification or mobility shifters. However, for the miRNAs having identical number of nucleotides (similar charge to size ratios), their respective PNA–miRNA hybrids would require mobility shifters, such as peptide-drag tags (earlier used in first generation DQAMmiR) for their resolution. Therefore, Liang modified the developed model for multiple miRNAs (with/without difference in number of nucleotides) by applying the effect of peptide drag tags on the electrophoretic mobility of the PNA–miRNA hybrids, as for now equation (12) could be rewritten as;

$$F_{\mathrm{E,hyb}} = F_{\mathrm{f,hyb}} + F_{\mathrm{f,tag}} \tag{16}$$

The hydrodynamic force, $F_{\mathrm{f.tag}}$, acting on the peptide drag tag could be expressed as;

$$F_{\mathrm{f,tag}} = 6\pi\eta R_{\mathrm{H,tag}} u_{\mathrm{rel}} \tag{17}$$

The hydrodynamic radius of the peptide drag tag, $R_{\mathrm{H,tag,}}$ could be derived by number of amino acid (aa) residues on the peptide drag tag [137], N_{tag} as:

$$R_{\mathrm{H,tag}} = (0.22 \pm 0.11) N_{\mathrm{tag}}^{0.57\pm0.02} \tag{18}$$

Substituting $F_{\mathrm{E,hyb}}$, $F_{\mathrm{f,hyb,}}$ and $F_{\mathrm{f.tag}}$ from equations (9), (10) and (17), respectively, in equation (16) and simplifying for electrophoretic mobility of PNA–miRNA hybrids with peptide drag tag, $\mu_{\mathrm{hyb+tag}}$,:

$$\mu_{\mathrm{hyb+tag}} = \frac{e}{2\pi z_i \eta \lambda_B}\left[\left(\ln\frac{2N_{\mathrm{hyb}}b}{d_{\mathrm{hyb}}} - 0.72\right)^{-1} + \frac{3R_{\mathrm{H,tag}}}{N_{\mathrm{hyb}}b}\right]^{-1} \tag{19}$$

Using final expression (equation (19)), the electrophoretic mobility calculation of PNA–miRNA hybrids with/without peptide drag tags can be determined. For instance, in case of 20-nts PNA–miRNA hybrids, the mobility shift using different length peptide drag tags was simulated in the following electropherogram **(Figure 13).**

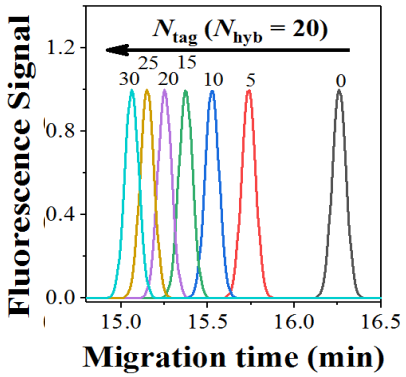

Figure 13: Simulated electropherogram for 20-nts PNA–miRNA hybrids using peptide drag of different number of amino acid residues (0, 5, 10, 20 and 30 amino acid residues). Migration times of peaks shown above were estimated by using $\mu_{EOF} = 3.14 \times 10^{-4}$ $cm^2 \cdot V^{-1} \cdot s^{-1}$ which was experimentally measured for the CE-run buffer containing 20 mM borax and 20% (v/v) acetonitrile at pH 9.0.

The theoretical mobility calculated for individual PNA–miRNA hybrids (18–25 nts) with and without drag tags using equation (19) are listed in Table:

Table 2: The estimated electrophoretic mobility ($cm^2 \cdot V^{-1} \cdot s^{-1}$) for PNA–miRNA hybrids with different number of base pairs (18–25 nts) and different-length peptide drag tags (0, 5, 10, 15, 20, 25 and 30 aa).

N_{tag} →

N_{hyb} ↓	0	5-aa	10-aa	15-aa	20-aa	25-aa	30-aa
18	5.37×10^{-5}	5.02×10^{-5}	4.86×10^{-5}	4.75×10^{-5}	4.65×10^{-5}	4.57×10^{-5}	4.49×10^{-5}
19	6.95×10^{-5}	6.40×10^{-5}	6.16×10^{-5}	5.99×10^{-5}	5.84×10^{-5}	5.72×10^{-5}	5.61×10^{-5}
20	8.45×10^{-5}	7.69×10^{-5}	7.36×10^{-5}	7.13×10^{-5}	6.93×10^{-5}	6.77×10^{-5}	6.62×10^{-5}
21	9.88×10^{-5}	8.89×10^{-5}	8.48×10^{-5}	8.18×10^{-5}	7.94×10^{-5}	7.73×10^{-5}	7.55×10^{-5}
22	1.12×10^{-4}	1.00×10^{-4}	9.54×10^{-5}	9.17×10^{-5}	8.88×10^{-5}	8.64×10^{-5}	8.43×10^{-5}

23	1.25×10^{-4}	1.11×10^{-4}	1.05×10^{-4}	1.01×10^{-4}	9.77×10^{-5}	9.49×10^{-5}	9.24×10^{-5}
24	1.38×10^{-4}	1.21×10^{-4}	1.15×10^{-4}	1.10×10^{-4}	1.06×10^{-4}	1.03×10^{-4}	1.00×10^{-4}
25	1.50×10^{-4}	1.31×10^{-4}	1.24×10^{-4}	1.19×10^{-4}	1.14×10^{-4}	1.11×10^{-4}	1.08×10^{-4}

Everything taken into account, the applicability of theoretical model for multiple miRNAs analysis was based on two logistics: 1) for miRNAs differing in N_{hyb}, their respective PNA–miRNA hybrids could be CE-separated without the need of peptide drag tags, 2) for miRNAs with identical N_{hyb}, their respective PNA–miRNA hybrids could be CE-separated by attaching different length peptide drag tags to complementary PNA probes. These logistics were then verified by performing a set of experiments for detection, separation and quantification of three human miRNAs simultaneously, out of which one had 22-nts (miRNA-21) and the other two had identical number of nucleotides, 20-nts (miRNA-378g and miRNA-147a), with 5-aa peptide drag tag attached to PNA probe complementary to miRNA-147a.

2.4.3 Materials and Methods

2.4.3.1 MiRNAs and complementary PNA probes. The miRNAs (miRNA-21: 5'-UAG-CUU-AUC-AGA-CUG-AUG-UUG A-3', miRNA- 378g: 5'- ACU-GGG-CUU-GGA-GUC-AGA-AG -3', and miRNA-147a: 5'-GUG-UGU-GGA-AAU-GCU-UCU-GC-3') were custom-synthesized by IDT (Coralville, IA, USA) and their respective fluorescently labeled PNA probes (Alexa488-O-5'-TCA-ACA-TCA-GTC-TGA-TAA-GCT-A-3', Alexa488-O-5'-CTT-CTG-ACT-CCA-AGC-CCA-GT-3', and Alexa488-O-5'-GCA-GAA-GCA-TTT-CCA-CAC-AC- 3'–Gly-Ala-Gly-Thr-Gly) were custom-synthesised by PNA Bio, Inc. (Newbury Park, CA). The other chemicals were obtained from Sigma-Aldrich (Oakville, ON, Canada) unless stated otherwise.

2.4.3.2 Hybridization Conditions. The hybridization reaction was performed in Mastercylcer 5332 thermocycler (Eppendorf, Hamburg, Germany). Various concentrations of different miRNAs were incubated with constant 10 nM of their respective PNA probes in CE-running buffer. The temperature was increased to a denaturing 95 °C and then lowered to 60 °C at the rate of 20 °C/minute and was held to 60°C for 30 min to allow annealing. In order to minimize miRNA degradation, a nuclease-free environment was maintained.

2.4.3.3 CE-LIF. All experiments were performed using a P/ACE MDQ CE instrument (Beckman-Coulter, Fullerton, CA, USA) equipped with a LIF detector. A 488 nM line of continuous wave solid-state laser (JDSU, Santa Rosa, CA, USA), with 1 mW effective output was utilized to excite fluorescently labeled probe. Fluorescence signal was detected at 520 nM wavelength. A bare fused-silica capillary with an outer diameter of 365 μm, an inner diameter of 50 μm, and a total length of 80 cm was used. The distance from the injection end of the capillary to the detector was 70 cm. Prior to each run, the capillary was flushed with 0.1M HCl, 0.1 M NaOH, deionized H_2O and the running buffer (20 mM borax 20% (v/v) acetonitrile pH 9.0) for 2 minutes each. Samples were injected at the positive end by a pressure pulse of 0.5 psi for 5seconds; the volume of the injected sample was ~ 6 nL. Electrophoresis was driven by electric field of 312.5 V/cm applied voltage and at coolant controlled temperature 20 °C. The resulting electropherograms were analysed using 32 Karat software. Peak areas were divided by the corresponding migration time to compensate for the dependence of the residence time in the detector in the electrophoretic velocity of analyte.

2.4.3.4 Spectrophotometric Determination of Target and Probe Concentrations. The target and probe concentrations were determined by light absorption at 260 nm using the Nano-Drop ND-1000 spectrophotometer (Thermo-Fisher Scientific). The stock concentration of the target

and probe was too high to measure directly; therefore, a small sample of the each stock solution was serially diluted, and absorbance of each sample at 260 nm was measured 3 times. The concentration of each sample was determined as ***absorbance*/εl** where ε is the molar extinction coefficient of the miRNAs and PNA probes at 260 nm respectively (provided by IDT/PNA Bio) and *l* is the optical path length. Using the concentrations of the serial dilutions, the original stock concentration was extrapolated.

2.4.4 Result and Discussion

2.4.4.1 Separation of three PNA–miRNA hybrids in CE. For the proof of principle study and to validate the two above-stated logistics, three miRNAs were selected, such that two had identical N_{hyb} (20-nts; miRNA-378g and miRNA-147a) and the third one had different N_{hyb} from the former two (22-nts; miRNA-21). We prospected that since miRNA-21(23-nts) had different and highest N_{hyb}; therefore, it could be separated from other two without any modification or mobility shifters (peptide drag tag) and, respectively would display the lowest electrophoretic mobility. With concerns to the miRNAs with identical N_{hyb} (miRNA-378g and miRNA-147a), we made use of custom synthesized PNA-peptide probe (5-aa residue attached to PNA probe) complementary to miRNA-147a, in order to separate PNA–miRNA-147a (20-nts) and PNA–miRNA-378g (20-nts). The peptide tag to PNA probe complementary miRNA-147a acted as a drag and shifted the peak of formed PNA–miRNA-147a (20-nts) towards left (highest electrophoretic mobility), away from PNA–miRNA-378g (20-nts) resolving the two peaks. The experiments were performed in CE run buffer containing 20 mM borax and 20% (v/v) acetonitrile at pH 9.0 for all three hybrid mixture injected at sample inlet. The experimental calculated electrophoretic mobility was compared with the theoretically estimated mobility for individual hybrids (PNA–miRNA-147a, -378g and -21), there was error of 29%, 26% and 6%, respectively (these errors corre-

sponds to discrepancies in the theoretical estimation of CE-mobility to that obtained experimentally) and also, in experiments, the PNA–miRNA-147a and -378g hybrid peaks were not baseline separated in CE (**Figure 14**). This concluded that 5-amino acid peptide drag tag was not sufficient to baseline separate miRNAs with identical N_{hyb}.

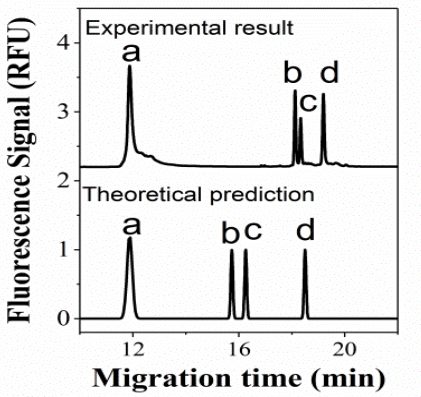

Figure 14: Discrepancies between the experimental and the predicted separation of three PNA–miRNA hybrids in 20 mM borax 20% (v/v) acetonitrile pH 9.0. Peak assignment: (a) excess PNA probes, (b) PNA–miR-147a (20-nts, 5aa), (c) PNA–miR-378g (20-nts), and (d) PNA–miR-21 (22-nts).

The reduction of EOF in CE is well-known to improve resolution for poorly resolved peaks. One such approach to suppress EOF is by increasing ionic strength of the run buffer, $\mu_{\mathbf{EOF}\ \alpha\ \frac{1}{\sqrt{\mathbf{ionic\ strenth}}}}$ [138], hence; we optimize the ionic strength by the addition of NaCl (0, 50, 100, and 120 mM) with the objective to baseline separate PNA–miRNA-147a and -378g hybrids (**Figure 15**). The resolution was calculated to track the effect after each sequential addition (**Table 3**). The addition of NaCl suppressed the EOF and increased the run time. At 120 mM NaCl in running buffer, PNA–miRNA-147a and -378g hybrids peak were found to be well resolved (Resolution: 3.1) and baseline separated. Therefore, the following CE experiments were performed using 20 mM borax 120 mM NaCl 20% (v/v) acetonitrile pH 9.0 as the run buffer.

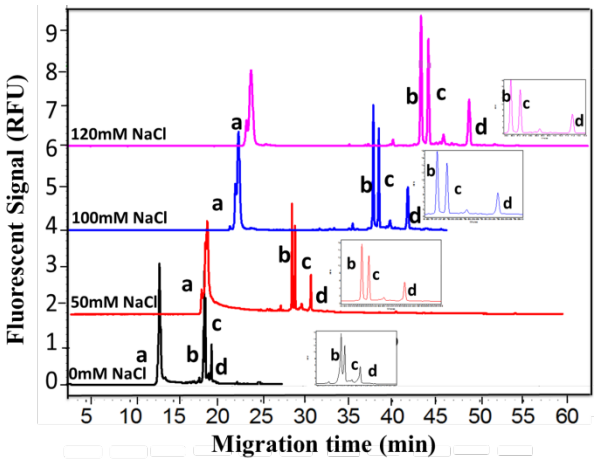

Figure 15: Achieving baseline separation of the three hybrids from each other by increasing the ionic strength of CE running buffer *via* addition of NaCl (0, 50, 100, 120 mM); At 20 mM borax **120 mM NaCl**, 20% (v/v) acetonitrile, pH 9.0, the hybrids peak were well-resolved (Resolution = 3.1). Peak assignment: (a) excess PNA probes, (b) PNA–miR-147a (20-nts, 5-aa), (c) PNA–miR-378g (20-nts), and (d) PNA–miR-21 (22-nts). Black, red, blue and pink trace represents the addition of 0, 50, 100, 120 mM NaCl in 20 mM borax 20% (v/v) acetonitrile, pH 9.0, respectively.

Table 3: Resolution between the PNA–miRNA-147a (20-nts, 5-aa) and PNA–miRNA-378g **(**20-nts**)** at different NaCl concentrations in CE-running buffer. Standard deviations from mean values were obtained from three experiments.

NaCl concentration (mM) in 20 mM borax 20% (v/v) acetonitrile pH 9.0	**Resolution**
0	3.1 ± 0.03
50	2.77 ± 0.01
100	2.27 ± 0.01
120	1.27 ± 0.02

2.4.4.2 Quantification of three miRNAs. The final investigation for the applicability of PNA-facilitated DQAMmiR in miRNA multiplexing studies was to simultaneously and accurately quantify all three miRNAs at different concentrations.

2.4.4.2.1 Determination of individual (q_H) and relative quantum yield (q_P) of the PNA probes complementary to three miRNAs. For accurate quantification of miRNAs, two considerations were taken into account; 1) individual quantum yield, q_H of PNA-miRNA hybrids probes with respect to their unbound probes and, 2) relative quantum yield, q_P of the probes (signifies the potential difference of quantum yields between the individual probes). The q_H was determined following the previously described expression for a single miRNA analysis. For determination of q_P, the fluorescence intensities of individual probe were normalized by calculating its relative quantum yield to PNA probe complementary to miRNA-21 (used as the normalization factor) as shown in **Figure 16.** The **Table 4** list the calculated q_H and q_P values:

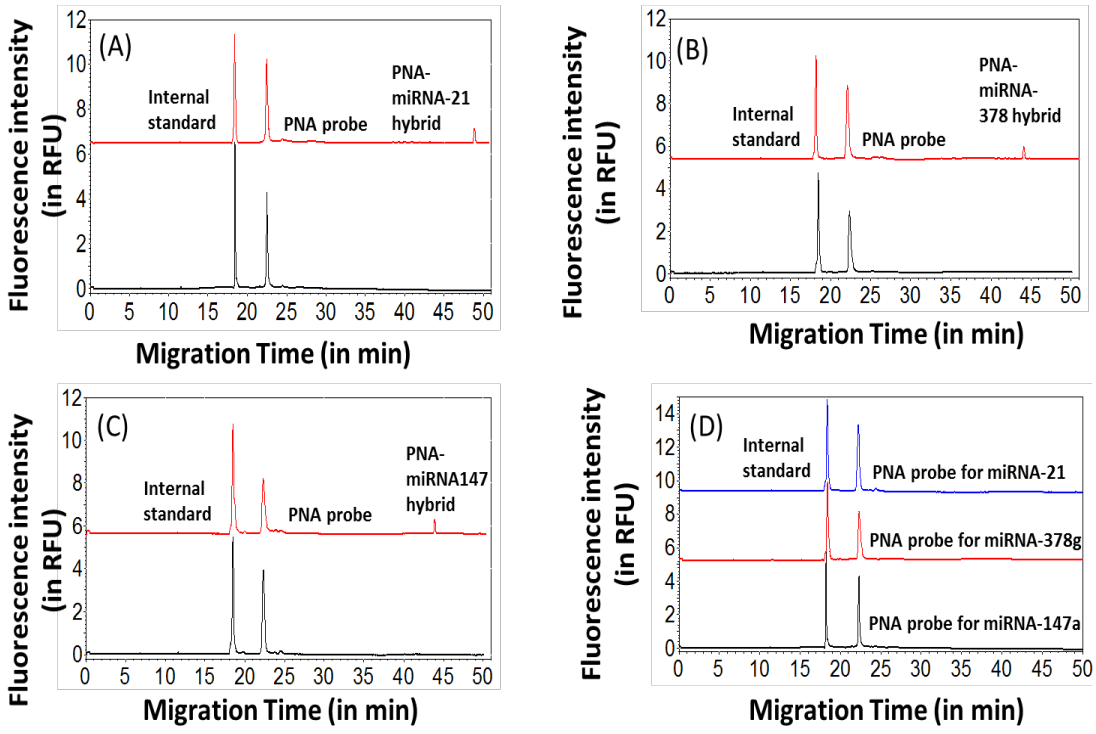

Figure 16: CE-LIF-facilitated determination of q_H and q_P for individual PNA probes using rhodamine as internal standard. (A) q_H for PNA probe complementary to miR-21; black trace with no target, red trace with target. (B) q_H for PNA probe complementary to miR-378g; black trace with no target, red trace with target. (C) q_H for PNA probe complementary to miR-147a; black trace with no target, red trace with target. (D) q_P determination with respect to PNA probe for miR-21; PNA probes complementary to miR-21, 378g and 147a are represented by black trace, red and blue trace respectively.

Table 4: Quantum yields of PNA–miRNA hybrids (q_H) to their unbound PNA probes and Relative quantum yields of the PNA probes (q_P) to the PNA probe corresponding/complementary to miR-21 for signal normalization. Standard deviations from mean values were obtained from three experiments.

	PNA probe complementary to		
	miRNA-147a	**miRNA-378 g**	**miRNA-21**
q_H	0.26 ± 0.01	0.34 ± 0.05	0.27 ± 0.02
q_P	0.82 ± 0.04	0.78 ± 0.04	1

2.4.4.2.2 Expression for quantification of multiple miRNAs using PNA-facilitated DQAM-miR. The unknown concentration of the *i*-th miRNA, [miRNA]$_i$, could be expressed through the area of its respective hybrid peak, $A_{H,i}$, using the unknown coefficient a, and known quantum yields $q_H{}^i$ and $q_P{}^i$:

$$[\text{miRNA}]^i = a\left(\frac{A_{\text{H}}^i}{q_{\text{H}}^i q_{\text{P}}^i}\right) \tag{20}$$

The known concentration of the *i*-th probe, $[\text{P}]_{0,I}$, could be expressed through two peak areas, $A_P{}^i$ and $A_H{}^i$, corresponding to unbound PNA probe and miRNA-bound probe, respectively, with the same coefficient a and the known quantum yield $q_H{}^i$ and $q_P{}^i$:

$$[\text{P}]_{0,i} = a\left(\frac{A_{\text{P}}^i}{q_{\text{P}}^i} + \frac{A_{\text{H}}^i}{q_{\text{H}}^i q_{\text{P}}^i}\right) \tag{21}$$

$$q_{\text{P}}^i[\text{P}]_{0,i} = a\left(A_{\text{P}}^i + \frac{A_{\text{H}}^i}{q_{\text{H}}^i}\right) \tag{22}$$

Similarly, for N, number of probes and hybrids,

$$\sum_{i=1}^{N}\left(q_{\text{P}}^i[\text{P}]_{0,i}\right) = a\left(\sum_{i=1}^{N} A_{\text{P}}^i + \sum_{i=1}^{N}\frac{A_{\text{H}}^i}{q_{\text{H}}^i}\right) \tag{23}$$

For the above expression, the corresponding peak area for individual hybrid ($A_H{}^i$) could be determined experimentally and, the unbound PNA probe came out in form of overlapped peaks due to similar mobilities and therefore, their cumulative peak area ($A_P{}^i$) could be expressed as $A_{\text{P}} = \sum_{i=1}^{N} A_P^i$ and below equation can be obtained:

$$\sum_{i=1}^{N}\left(q_{\mathrm{P}}^{i}[\mathrm{P}]_{0,i}\right)=a\left(A_{\mathrm{P}}+\sum_{i=1}^{N}\frac{A_{\mathrm{H}}^{i}}{q_{\mathrm{H}}^{i}}\right) \tag{24}$$

Here, a can be expressed as;

$$a=\frac{\sum_{i=1}^{N}\left(q_{\mathrm{P}}^{i}[\mathrm{P}]_{0,i}\right)}{A_{\mathrm{P}}+\sum_{I=1}^{N}\frac{A_{\mathrm{H}}^{i}}{q_{\mathrm{H}}^{i}}} \tag{25}$$

By substituting a from equation (25) to equation (24), the final equation (26) was derived to quantitate i-th miRNA from a single electropherogram without plotting a calibration curve

$$[\mathrm{miRNA}]^{i}=\frac{A_{\mathrm{H}}^{i}}{q_{\mathrm{H}}^{i}q_{\mathrm{P}}^{i}}\frac{\sum_{i=1}^{N}\left(q_{\mathrm{P}}^{i}[\mathrm{P}]_{0,i}\right)}{A_{\mathrm{P}}+\sum_{i=1}^{N}\frac{A_{\mathrm{H}}^{i}}{q_{\mathrm{H}}^{i}}} \tag{26}$$

In final expression (equation (26)), $[\mathrm{P}]_0{}^i$ is the total concentration of the i-th PNA probe (composed of the unbound and the target-bound probe), $A_{\mathrm{H}}{}^i$ is the area corresponding to the i-th hybrid, A_{P} is the cumulative area of the unbound probes, $q_{\mathrm{P}}{}^i$ is a relative quantum yield of the i-th PNA probe to normalize the quantum yield differences between the probes, and $q_{\mathrm{H}}{}^i$ is the relative quantum yield of the i-th hybrid with respect to that of the unbound probe. Both $q_{\mathrm{P}}{}^i$ and $q_{\mathrm{H}}{}^i$ were determined in separate experiments.

2.4.4.2.3 5-point quantification for multiple miRNAs. The different concentration miRNAs (500, 250, 125, 62.5, and 31.25 pM) were incubated with constant concentration of their respec-

tive PNA/PNA-peptide probes (10 nM) in the same vial for hybridization and thereafter, the formed hybrids were CE analysed (**Figure 17**).

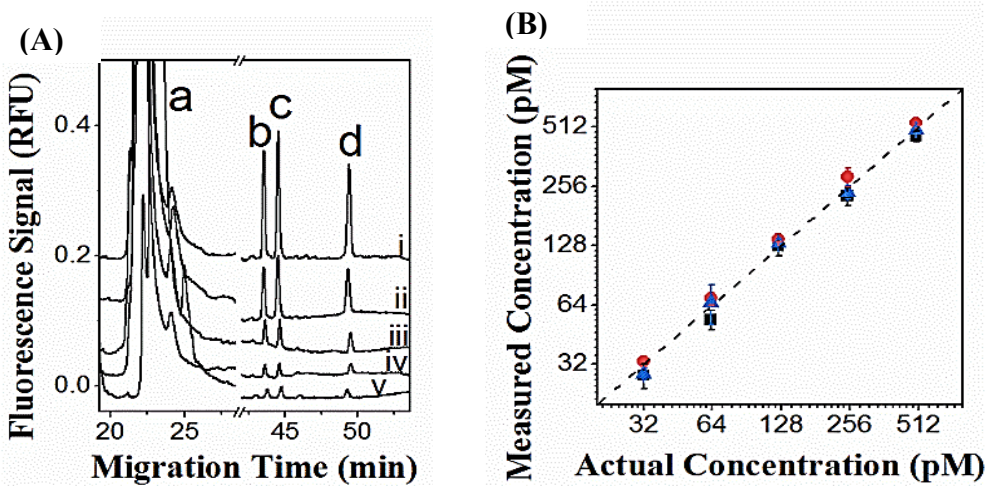

Figure 17: A) CE-Electropherograms of PNA-facilitated DQAMmiR measurements. Peak assignment: (a) excess PNA probes, (b) PNA–miR-147a (20-nts, 5-aa), (c) PNA–miR-378g (20-nts), (d) PNA–miR-21 (22-nts). Electropherograms i–v correspond to target concentrations of 500, 250, 125, 62.5, and 31.5 pM, respectively. **B)** Quantitation plot between PNA-facilitated DQAMmiR measured concentrations and spectroscopically determined concentration at 260 nm for three miRNAs simultaneously. miRNA-21, miRNA-147a, and miRNA-378g, are represented by black rectangles, red circles, and blue triangles, respectively. The dashed line (y = x) represents a line corresponding to 100% recovery. Error bars represent standard deviation from mean values obtained from three experiments.

The accuracy of the assay was determined by comparing the PNA-facilitated DQAMmiR concentration to the spectroscopically determined miRNA concentrations at 260 nm. A recovery between 90–110% and relative standard deviation (RSD) of <15% was observed for all three miRNAs analysed simultaneously (**Table 5**). In addition, we determined limit of detection (LOD) for our assay as 14 pM by studying signal to noise ratio (S/N) of the hybrid peaks.

Table 5: Quantification results obtained from PNA-facilitated DQAMmiR for three miRNAs (miRNA-147a, miRNA-378g and miRNA-21) corresponding to their actual concentrations as determined spectroscopically at 260 nm. Standard deviations and recovery from mean values were obtained from three experiments.

Actual miRNA Concentration (pM)	**DQAMmiR-Measured miRNA Concentration (pM, Mean ± Standard Deviation) & % Recovery**					
	miR-21		**miR-147a**		**miR-378g**	
	Concentration (in pM)	% Recovery	Concentration (in pM)	% Recovery	Concentration (in pM)	% Recovery
500	461 ± 28	92	538 ± 11	107	483 ± 17	97
250	229 ± 25	91	287 ± 30	114	240 ± 19	96
125	128 ± 14	102	138 ± 4	110	118 ± 6	94
62.5	59 ± 6	94	69 ± 5	110	60 ± 15	96
31.25	29 ± 4	93	33 ± 2	101	33 ± 2	106

2.4.5 Conclusion

Here, we introduced and developed the second generation DQAMmiR which is, in principle, more simpler and robust than first generation DQAMmiR, as it omits the addition of external mobility modifier (*e.g.,* SSB) to separate the excess unbound hybridization probes from the formed hybrids. The assay employs the use of PNAs, which are neutral polymer, capable of hybridizing with the miRNAs at accelerated rate (due to lack of repulsion) and as being charge-neutral render electrophoretic mobility different from the partial-negatively charged PNA–miRNA hybrids (due to negative charge on miRNAs) separating the excess unbound PNA probes and the formed PNA–miRNA hybrids. Yet, PNA-facilitated DQAMmiR, like first generation, requires peptide drag tags and optimal CE conditions for the separation of similar mobility hybrids (miRNAs having identical N_{hyb}). Following this, we simultaneously quantified three

miRNAs with recovery in between 90–110%, RSD <15% and LOD ~14 pM using commercial CE setting. The accuracy, precision and sensitivity of our assay suggested its potential use for cost-effective analysis of known clinically relevant miRNAs in basic laboratory settings.

Chapter Three

VALIDATION OF PNA-FACILITATED DQAMmiR IN CRUDE CELL LYSATE

3.1 Background

MiRNAs have well-proven their significance as a promising diagnostic and prognostic cancer biomarkers. Despite of their exceptional potential, the clinical quantification of miRNAs is technically challenging due to their low abundance, small size and high sequence homology. Though there are currently numerous established methods that dissert their clinical potential to be sensitive and specific, such as well-known gold standard RT-qPCR, Nanostring, deep sequencing, *etc*.; however, with regards to their respective shortcomings, the demand to develop a simple, robust and multiplexable quantitative miRNA detection assay still persists. Moreover, most of the existing techniques essentially require sample processing and RNA extraction, which is, in turn challenging and typically rate-limiting. The available commercial and in-house reagents commonly used for RNA isolation are more or less prone to variability in quantification data (decreasing the reliability of the assay) and also, there no standardization/normalization procedure to follow for the same. In addition, these reagents overall increases the assay cost and are not easily feasible [74, 139, 140].

Our lab had introduced PNA-facilitated DQAMmiR which is advantageous, importantly, for its direct approach, *i.e.*, does not require RNA extraction/amplification. This reduces the extraction- and amplification-based biases and facilitates reliable absolute quantification of multiple miRNAs simultaneously. Briefly, it is a hybridization assay which involves the use of un-

charged PNA probes, in excess (to reduce the hybridization time) to hybridize with the complementary miRNAs in solution and subsequent separation of the formed hybrids from each other (using peptide-drags) and from excess probes (charge difference) in commercial CE-LIF settings. The absolute quantification of individual miRNA is achieved using mathematically derived expression by equating the experimentally determined variables. The earlier work demonstrated the assay potential of being sensitive, accurate (RSD <10%) and robust for relatively cost-effective miRNAs analysis. In addition, CE-LIF provides sensitive and specific analysis of trace biomolecules in complex sample matrices such as cell lysates, tissues and various biofluids [92, 93]. Previously, the first generation DQAMmiR had proved its robustness in analysing miRNAs, irrespective of sample matrices, by performing comparative studies for single miRNA in pure buffer and crude cell lysate.

Prostate cancer (PCa) is the second most commonly diagnosed cancer in men worldwide and it is the fifth leading cause of cancer-related death [141]. However, the most important clinical challenge in its diagnosis is to distinguish men who have potentially lethal form of PCa from those with an indolent (slow-growing) disease [142]. Presently, the stratification of PCa patient is guided by the PSA (prostate specific antigen) kinetics, clinical stage, and Gleason score (tumor grade). Though these parameters are helpful, these have limitations in detecting cases, predicting disease outcomes and in guiding clinical management. Hence, new biomarkers are pressingly needed to overcome the limitation of existing diagnostic and prognostic approaches. Studies revealed the dysregulated miRNAs expressions in PCa and their potential of being employed as biomarkers for diagnosis [143].

Here we demonstrate the multiplexed quantification of endogenously-present miRNAs directly from crude PCa cell-lysate without isolating RNA, using PNA-facilitated DQAMmiR.

For this work, we selected two known prostate cancer specific dysregulated miRNAs; miRNA-20b and miRNA-100. MiR-20b has reported to be strongly overexpressed in cancerous tissues compared to the normal prostate tissues; it acts as oncogene and promotes cellular proliferation and migration by directly regulating phosphatase and tensin homolog in prostate cancer [144]. MiRNA-100 act as tumor-suppressor, downregulation of which enhances migration, invasion and transition properties in PCa cells [145]. The use of appropriate lysis buffer made it possible to liberate miRNAs from the cells and from the carrier protein for the accurate analysis. In this respect, an assay validation procedure was designed to observe the CE pattern in presence of pure buffer and crude cell lysate. As a part of which, we employed standard addition approach to determine the miRNAs concentration in prostate cancer cell by adding known concentrations of respective prostate cancer-related miRNAs in cell lysate and pure buffer and generating the respective standard addition plots. The accurate miRNA detection and quantification in PCa cell line would get our assay a step closer to its clinical implementation to actual patient-derived samples in diagnostic settings.

3.2 Material and Methods

3.2.1 MiRNAs and complementary PNA probe. The miRNAs (miR-20b: 5'- CAA-AGU-GCU-CAU-AGU-GCA-GGU-AG -3', miR-100: 5'- AAC-CCG-UAG-AUC-CGA-ACU-UGU-G-3') was custom-synthesized by IDT (Coralville, IA, USA) and their respective fluorescently labeled PNA probe (Alexa 647-O-O-5'- CTA-CCT-GCA-CTA-TGA-GCA-CTT-TG -3', Alexa 647-O-O-5'- CAC-AAG-TTC-GGA-TCT-ACG-GGT-T -3`–Gly-Thr-Gly-Ala-Gly) was cus-

tom-synthesised by Panagene, Inc. (Yuseong-gu, Daejeon, Korea).The other chemicals were obtained from Sigma-Aldrich (Oakville, ON, Canada) unless stated otherwise.

3.2.2 Hybridization Conditions. The hybridization reaction was performed in Mastercylcer 5332 thermocycler (Eppendorf, Hamburg, Germany). Various concentrations of different miRNAs were incubated with constant 10 nM of their respective PNA probes in CE-running buffer and cell lysate. The temperature was increased to a denaturing 95 °C and then lowered to 60 °C at the rate of 20 °C/minute and was held to 60°C for 30 min to allow annealing. In order to minimize miRNA degradation, a nuclease-free environment was maintained.

3.2.3 CE-LIF. All experiments were performed using a P/ACE MDQ CE instrument (Beckman-Coulter, Fullerton, CA, USA) equipped with a LIF detector. A 641 nm line of continuous wave solid-state laser (JDSU, Santa Rosa, CA, USA), with 1 mW effective output was utilized to excite fluorescently labeled probes. Fluorescence signal was detected at 679 nm wavelength. A bare fused-silica capillary with an outer diameter of 365 μm, an inner diameter of 75 μm, and a total length of 80 cm was used. The distance from the injection end of the capillary to the detector was 70 cm. Prior to each run, the capillary was flushed with 0.1M HCl, 0.1 M NaOH, deionized H2O and the running buffer (20 mM borax 20% (v/v) acetonitrile pH 9.0) for 2 minutes each. Samples were injected at the positive end by a pressure pulse of 0.5 psi for 5seconds; the volume of the injected sample was ~ 6 nL. Electrophoresis was driven by electric field of 312.5 V/cm applied voltage and at coolant controlled temperature 20 °C. The resulting electropherograms were analysed using 32 Karat software. Peak areas were divided by the corresponding migration time to compensate for the dependence of the residence time in the detector in the electrophoretic velocity of analyte.

3.2.4 Spectrophotometric Determination of Target and Probe Concentrations. The target and probe concentrations were determined by light absorption at 260 nm using the Nano-Drop ND-1000 spectrophotometer (Thermo-Fisher Scientific). The stock concentration of the target and probe was too high to measure directly; therefore, a small sample of the each stock solution was serially diluted, and absorbance of each sample at 260 nm was measured 3 times. The concentration of each sample was determined as $absorbance/\varepsilon l$ where ε is the molar extinction coefficient of the miRNAs and PNA probes at 260 nm respectively (provided by IDT/PNA Bio) and l is the optical path length. Using the concentrations of the serial dilutions, the original stock concentration was extrapolated.

3.2.5 Prostate cancer cell culture and lysis. DU145 cells were obtained by Stanley K. Liu lab. The cell were grown in DMEM culture medium supplemented with 10% fetal bovine serum, 1% penicillin/streptomycin at 37 °C in a humidified environment of 5% CO_2, in air. Cells were harvested at 50-70% confluency using trysin/EDTA (0.25%/0.5 mM) and centrifuged at 5000 rpm for 5 min to form pellet. The washing of the formed pellets was done twice with 1XPBS. Subsequently, the cells were counted in hemocytometer. The cells were lysed in CE-running buffer containing 2% of SDS (sodium docyl sulphate). The cell lysate were aliquoted and stored at -80 °C.

3.3 Result and Discussion

We aimed to scale our assay to simultaneously and quantitatively analyse two PCa-dysregulated miRNAs in crude cell lysate without any RNA extraction. Since, a single miRNA biomarker might not be sufficient to study the state of the disease, hence, we analysed two PCa

dysregulated miRNAs (miR-20b, oncogene and miR-100, tumor-suppressor gene) having 23-and 22-nts, respectively. Similarly, two complementary PNA probes were employed with one conjugated with 5-aa peptide drag (to ensure sufficient separation of the two formed hybrids). Broadly, the work had two stages; 1) PCa cell lysis, and 2) miRNAs analysis by PNA-facilitated DQAM-miR.

3.3.1 Cell Lysis

MiRNAs display exceptional stability in physiological environment; however, miRNA is rarely found in free-state and is mostly either protein-bound (with RNA-binding protein, HDL) or enclosed in microvesicles and apoptotic bodies [15]. We performed alkaline lysis using high concentration (2%) of SDS in the incubation buffer (20 mM borax 20% (v/v) acetonitrile pH 9.0); to cause disruption of cell walls and denaturation of all protein associated with miRNAs for their efficient and complete release in cell-lysate. SDS is a strong anionic detergent and one of the most commonly used surfactant for cell-lysis in biochemical assays for rapid cell lysis on the order of seconds without the need of any special equipment [146].

3.3.2 Method Validation in presence of cell lysate

PNA as hybridization probes are well-known to be stable in degrading cellular environment, in comparison to usual DNA/LNA probe, due to its unnatural backbone (resistant to nuclease degradation). Moreover, PNA–RNA duplexes have reported to be more intact in degrading cellular environment than DNA–RNA or RNA–RNA duplexes [116, 147]. To perform quantitative analysis of miRNAs in PCa derived crude cell lysate, the respective PNA probes were added to the lysate at constant concentration and varying the concentrations of spike-in miRNAs following the earlier used hybridization protocol. In addition, similar PNA probe mixture and miR-

NA concentrations were also spiked-in pure buffer, in order to notice, if any, matrix effects. The hybridized sample was then injected to the capillary and CE-LIF analysed.

In our study, clinical validity of the method was attended taking into account the following criteria: ability to detect endogenous miRNA, accuracy, precision, linearity, limit of detection (LOD) and limit of quantification (LOQ). Furthermore, we performed cross-reactivity analysis of the probe in the presence of non-specific/cross miRNAs.

3.3.2.1 Detection of endogenous miRNA. To check the sensitivity of our assay in detecting endogenous miRNA, the respective probes (complementary to miRNA-20b and miR-100) were incubated in PCa cell lysate (1 million/ml), which was followed by CE analysis. With given conditions, we were able to detect one hybrid peak (electrophoretic mobility similar to PNA–miR-20). Further to identity the peak, the two miRNAs were subsequently spiked-in (at low concentration) to probes-cell lysate solution. From the result shown in **Figure 19, Table 6** we hypnotised the hybrid peak to be of miRNA-20. This indicated the potential ability of our assay to detect endogenous upregulated miRNA-20 without RNA extraction or miRNA amplification using commercial CE setting.

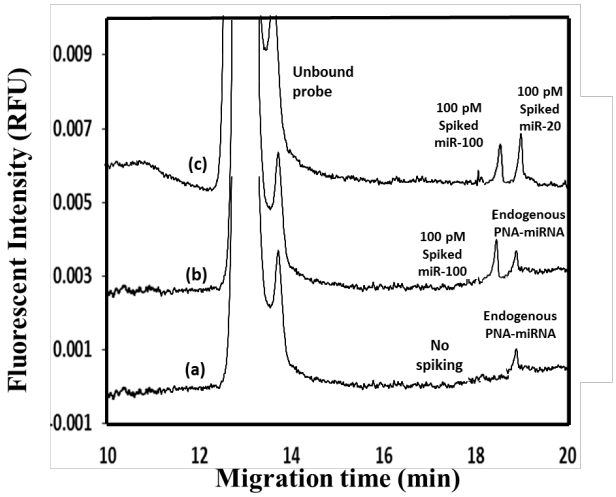

Figure 18: Detection of endogenous miRNA in PCa cell lysate (1 million/ml). (a) CE run for 1 nM PNA probes in cell lysate with no miRNA spiking; (b) CE run for 1 nM PNA probe mixture with spiked 100 pM miRNA-100; and (c) CE run for 1 nM PNA probe mixture with spiked 100 pM miRNA-100 and 100 pM miRNA-20.

Table 6: Detection and quantification of endogenous miRNA in PCa cell lysate (1 million/ml) by doing spike-in analysis. (a) 1 nM PNA probe mixture in cell lysate with no miRNA spiking (b) CE run for 1 nM PNA probe mixture with spiked 100 pM miRNA-100 (c) 1 nM PNA probe mixture with spiked 100 pM miRNA-100 and 100 pM miRNA-20. The experiment was done in duplicates

		Spiked-in Concentration (in pM)	Calculated Concentration (in pM)
(a)	**miRNA-100**	0	0
	miRNA-20	0	>LOD, <LOQ
(b)	**miRNA-100**	100	97.8
	miRNA-20	0	>LOD, <LOQ
(c)	**miRNA-100**	100	95.4
	miRNA-20	100	154.5

3.3.2.3 Accuracy. The obtained CE results were used to quantify the five different spike-in concentrations of the both miRNAs. The concentrations of the miRNAs were determined using (earlier derived) following equation:

$$[\text{miRNA}]^i = \frac{A_{\text{H}}^i}{q_{\text{H}}^i q_{\text{P}}^i} \frac{\sum_{i=1}^{N} \left(q_{\text{P}}^i [\text{P}]_{0,i} \right)}{A_{\text{P}} + \sum_{i=1}^{N} \frac{A_{\text{H}}^i}{q_{\text{H}}^i}}$$

Here, $[\text{P}]_0{}^i$ is the total concentration of the *i*-th PNA probe (composed of the hybrid and the excess probe), $A_{\text{H}}{}^i$ is the area corresponding to the *i*-th hybrid, A_{P} is the cumulative area of the unbound probes, $q_{\text{P}}{}^i$ is a relative quantum yield of the *i*-th PNA probe to normalize the quantum yield differences between the probes, and $q_{\text{H}}{}^i$ is the relative quantum yield of the *i*-th hybrid with respect to that of the unbound probe. Both $q_{\text{P}}{}^i$ and $q_{\text{H}}{}^i$ were determined in separate experiments (**Figure 19)** and listed in **Table 6**.

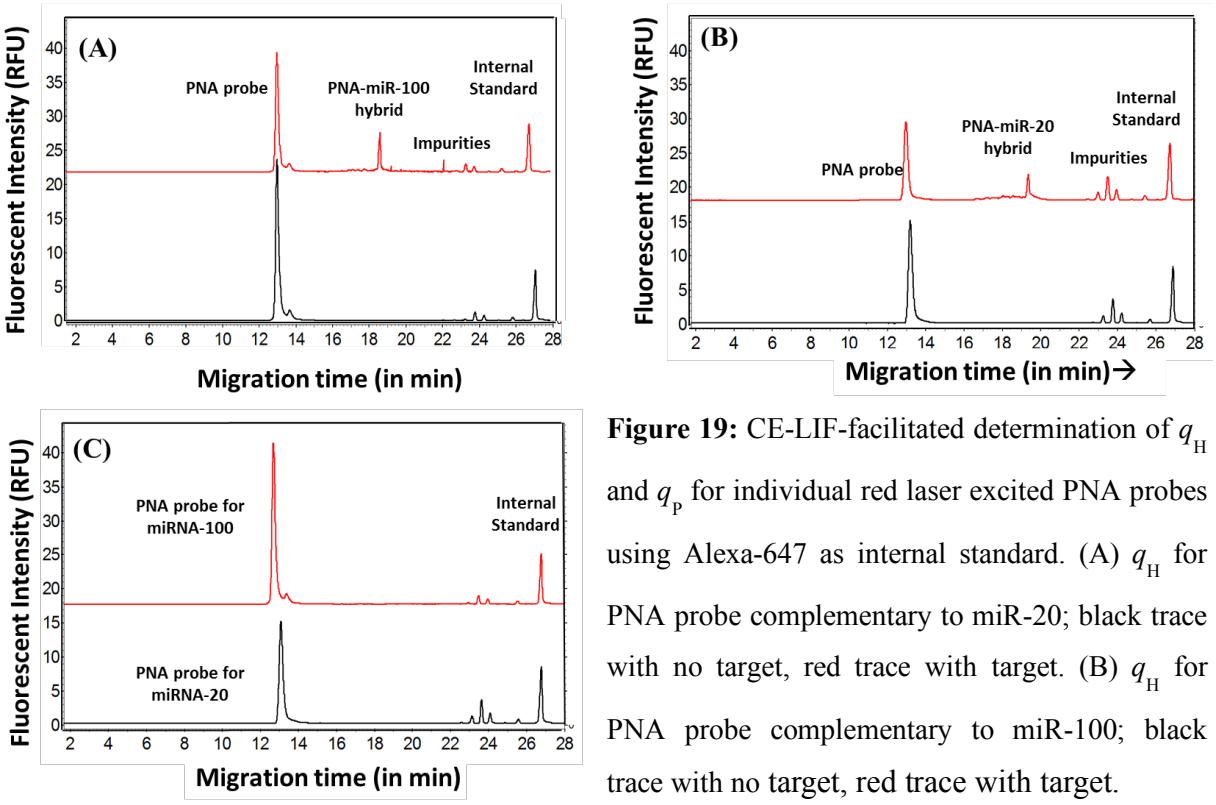

Figure 19: CE-LIF-facilitated determination of q_H and q_P for individual red laser excited PNA probes using Alexa-647 as internal standard. (A) q_H for PNA probe complementary to miR-20; black trace with no target, red trace with target. (B) q_H for PNA probe complementary to miR-100; black trace with no target, red trace with target. (C) q_P determination with respect to PNA probe for miR-20; PNA probes for miR-20 and 100 are represented by black trace and red trace respectively.

Table 7: Quantum yields of PNA–miRNA hybrids (q_H) to their unbound PNA probes and relative quantum yields of the PNA probes (q_P) to the PNA probe corresponding/complementary to miR-20 for signal normalization. Standard deviations from mean values were obtained from three experiments.

	PNA probe complementary to	
	miRNA-20a	**miRNA-100**
q_H	0.26 ± 0.01	0.28 ± 0.03
q_P	0.88 ± 0.02	1

Various concentrations of miRNAs (0, 0.125, 0.25, 0.5, 1, and 2 nM) were incubated with the constant concentration of PNA probes in pure buffer and in cell lysate. The formed hybrid were analysed in CE; and their respective concentrations were determined using earlier derived equation (**Figure 20**). The percentage recovery for all the concentrations for both miRNAs was between 90–113% and percentage error <15%, irrespective of matrix (**Table 7**).

Table 8: Quantification results obtained from PNA-facilitated DQAMmiR for two miRNAs (miRNA-20b and miRNA-100) corresponding to their actual concentrations as determined spectroscopically at 260 nm in presence of pure buffer and cell lysate. Standard deviations and percentage recovery (%) from mean values were obtained from three experiments.

Actual miRNA Concentration (nM)	DQAMmiR-Measured miRNA Concentration (nM), Mean ± Standard Deviation) and % Recovery							
	Pure buffer				Cell lysate			
	miR-20		miR-100		miR-20		miR-100	
	Concentration (nM)	% Recovery	Concentration (nM)	% Recovery	Concentration (nM)	% Recovery	Concentration (nM)	% Recovery
2	1.93 ± 0.07	96	1.89± 0.07	94	2.2 ± 0.05	107	2.17 ± 0.03	108
1	1.1 ± 0.04	110	1.01 ± 0.05	101	1.02 ± 0.03	98	0.97 ± 0.01	97
0.5	0.52 ± 0.01	104	0.49 ± 0.03	98	0.54 ± 0.02	98	0.51 ± 0.01	101
0.25	0.24 ± 0.01	96	0.23 ± 0.01	92	0.29 ± 0.01	97	0.26 ± 0.01	102
0.125	0.135 ± 0.005	107	0.138 ± 0.01	107	0.164 ± 0.01	93	0.142 ± 0.01	113
0	0	0	0	0	0.039± 0.005	-	<LOD	-

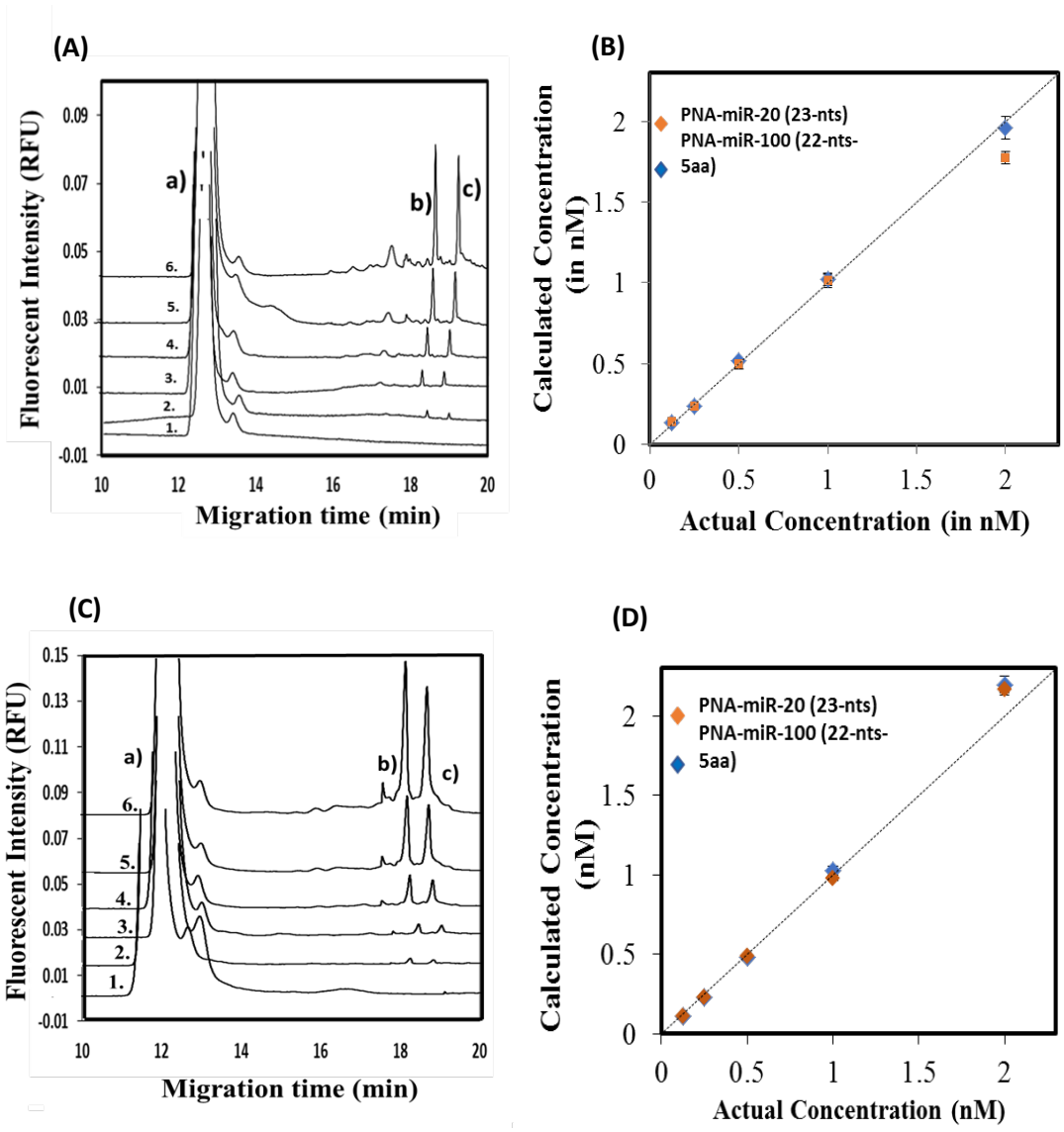

Figure 20: Spike-in recovery/ miRNA detection in CE in (A) pure buffer, and (C) cell lysate at different spiked-in concentrations. Electropherograms 1-6 correspond to miRNA concentrations of 0, 0.125, 0.25, 0.5, 1, and 2 nM, respectively. The 5- point calibration plot for different concentrations of miRNAs in (B) pure buffer, and (D) cell lysate. Error bars represents the standard deviations obtained from the mean of triplicate runs. Peak assignments: (a) unbound probe, (b) PNA–miR-100 (22-nts–5aa), and (c) PNA–miR-20 (23-nts).

2.2.3 Precision. Precision governs the quality of data, hence, good precision, as repeatability and inter-day precision is required to demonstrate the performance efficiency of the method. Repeatability was obtained from the analysis, during same day, of three replicates of three different concentrations for individual miRNA and coefficient of variation (CV) of all cases was obtained. The inter-day precision was determined by measuring standard curve (in triplicates) on two different days at low (0.125 nM), medium (0.5 nM) and high (2 nM) miRNA concentrations and hence, coefficient of variation was obtained. The CV was found to be <15% (**Table 8**) proving our assay to be precise.

Table 9: Coefficient of variation (%) for miRNAs in pure buffer and cell lysate (1 million/ml) for low (0.125 nM), medium (0.5 nM) and high (2 nM) miRNA concentration.

Actual miRNA Concentration (nM)	Coefficient of Variation (%)			
	Pure buffer		Cell lysate	
	miR-20	miR-100	miR-20	miR-100
2	3.63	2.2	2.32	1.6
0.5	2.73	6.21	5.83	6.94
0.125	3.98	6.8	6.18	7.69

3.3.2.4 Linearity. The 5-point standard addition curve was prepared by plotting five different spectroscopically determined and PNA-facilitated DQAMmiR calculated spiked-in concentrations of the individual miRNAs in the cell lysate. Linearity of the curve for each miRNA was verified by the coefficient of determination ($R^2 > 0.99$) and the coefficient of variation between the response factors (CV > 15%).

3.2.2.5 Limit of detection and Limit of quantification. The minimum concentration that provided a signal to noise ratio equal to 3 for both miRNAs was denoted limit of detection for our assay and the limit of quantification was set as the minimum concentration that gave signal to noise ratio equal to 10, whose average should not deviate beyond d ± 20% of the known actual concentration. The LOD and LOQ for our assay was measured by linear regression analysis and plotting signal to noise ratio plot between different concentration of both PNA–miRNAs in pure buffer and in cell lysate (**Figure 21**). The LOD and LOQ for respective miRNAs in presence of pure buffer and cell lysate are shown in **Table 9.**

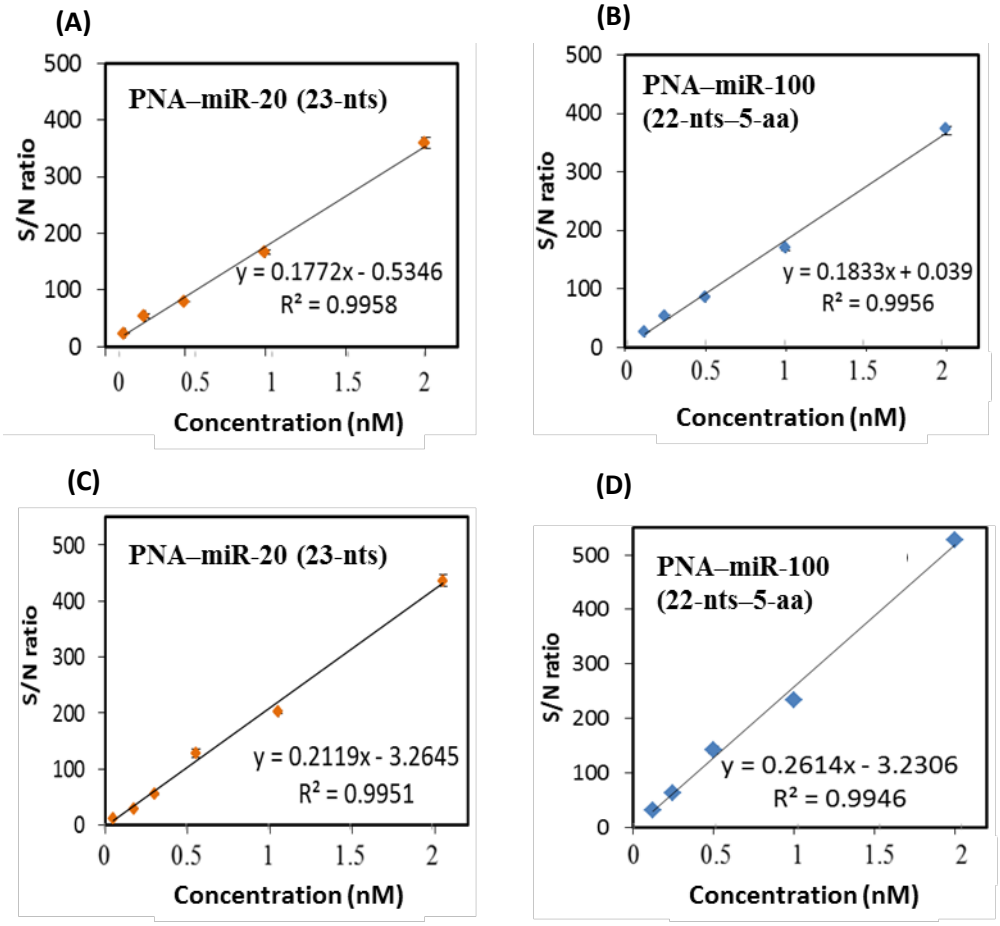

Figure 21: Signal to noise ratio plot in pure buffer for (A) PNA–miR-20 (23-nts), and (B) PNA–miR-100 (22-nts-5-aa); and in the presence of cell lysate for (C) PNA–miR-20 (23-nts), and (D) PNA–miR-100 (22-nts-5-aa) at different concentration. Error bars represents the standard deviations obtained in triplicate runs.

Table 10: Limit of detection and limit of quantification for individual miRNA obtained in presence of pure buffer and cell lysate

	Pure buffer		Cell lysate	
	miR-20	miR-100	miR-20	miR-100
LOD (in pM)	20	16	29	24
LOQ (in pM)	59	54	63	50

3.3.2.6 Cross-reactivity of the probe. In the physiological samples, there is not just the target miRNAs; rather multiple miRNAs with high sequence homology are present. With any miRNA hybridization assay, there is a wide variance in melting temperatures of the different hybrids. Each probe has a specific temperature at which specific miRNA binding occurs while non-specific binding does not. To test the specific behaviour of PNA-facilitated DQAMmiR, we incubated PNA probe complementary to miR-20b with miR-100 and vice-versa (**Figure 22**). The results justified that even at high probe and target concentration (ensures accelerated hybridization); neither of PNA probes showed any cross-reactivity to their non-specific miRNAs.

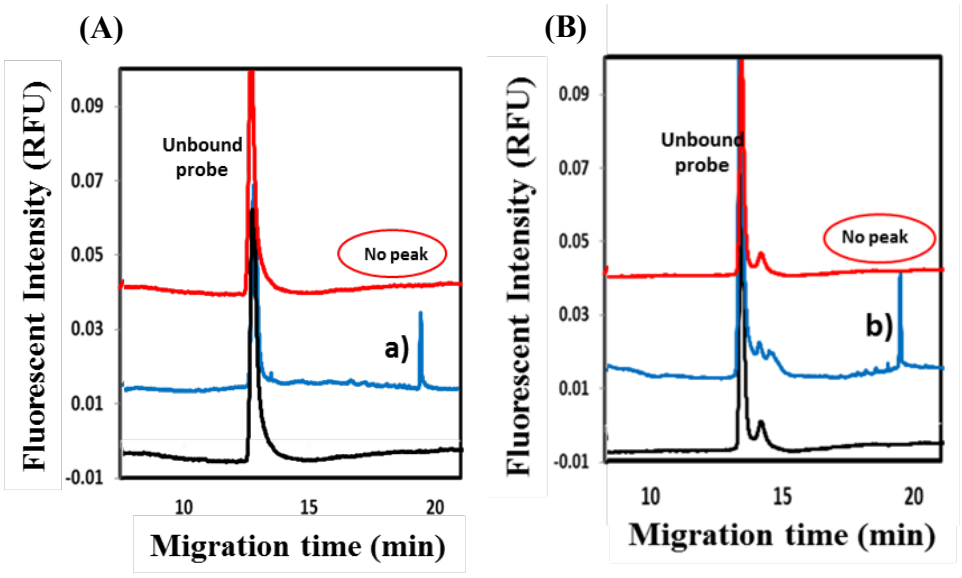

Figure 22: Cross-reactivity analysis for PNA probes; (A) CE run for10 nM PNA complementary to miR-20b incubated with: no target (black trace); 1 nM specific miR-20b (blue trace) ;and 1 nM non-specific miR-100 (red trace). (B) CE run for 10 nM PNA complementary to miR-100 incubated with: no target (black trace); 1 nM specific miR-100 (blue trace); and 1 nM non-specific miR-20b (red trace). Either of PNA probes shows no hybrid peak with non-complementary targets. Peak assignments: (a) PNA–miRNA-20 (23-nts), and (b) PNA–miRNA-100 (22-nts-5aa).

3.4 Conclusion

Here, we aimed to validate the feasibility of PNA-facilitated DQAMmiR in the presence of crude cell lysate derived from prostate cancer cell lines. The method fulfilled the general validation criteria for analytical technique including suitable level of linearity, low limit of detection and limit of quantification, good repeatability and reproducibility, and high recovery and accuracy; irrespective of sample matrix (pure buffer/cell lysate). Furthermore, with given conditions, we were able to detect an endogenous target (miRNA-20), which reported to be upregulated in prostate cancer, without any extraction and/or amplification. The success of the cell-lysate validation study is a milestone to scale our method to the clinical studies on patient-derived sample for miRNAs analysis.

LIMITATIONS

Though PNA-facilitated DQAMmiR is an improvement of our lab-developed first generation DQAMmiR, in the respect that this particular assay does not require any external mobility shifter (e.g., SSB) to resolve miRNA–bound probes from the excess unbound probes, owing to the neutral framework of PNA probes in comparison to partial negatively-charged PNA–miRNA hybrids; however, the particular also have its drawbacks. Firstly, the synthesis PNAs by itself is relatively more expensive than usual DNA/LNA probes, which overall increases the assay-cost. Secondly, being built on uncharged peptide chain (N-amino-ethyl-glycine units), PNA poses not only solubility problem (which affects its delivery into the solution), but also tends to adhere to the walls of capillary (during CE), which in turn leads to excess unbound PNA probes not reaching the detector. We tried to overcome this, by using PNA probes with O-linkers and addition of organic solvent (20% v/v acetonitrile) to all the working solutions/buffers. Thirdly and more critically, the presence of unnatural backbone, though this protects the PNA–miRNA hybrids from the enzymatic degradation, but the (non-ribose phosphate) backbone flexibility of PNA creates difficulty in the theoretical prediction of the PNA–miRNA hybrids mobility. The latter is important in multiplexing studies to design PNA/PNA–peptide probes. Our lab is still working to develop a more robust theoretical model to predict the hybrids mobility. Finally, the same inherent limitation of low sensitivity to detect very low abundance miRNAs in the physiological sample, similar to first generation DQAMmiR still persists. Ongoing work continues to develop an in-house CE detection set-up that potentially will reduce the LOD down to few hundreds copies of miRNAs, in practice.

CONCLUSION AND FUTURE WORK

The accurate quantification of miRNAs expression profile is crucial for understanding their prominent role in gene regulation and indeed to extend their clinical application as disease biomarkers. There are only a few methods which satisfy the criteria of accurate and reliable quantitation and facilitate multiplexing. One of such approaches was previously being developed by our lab is direct quantitative analysis of multiple miRNAs (DQAMmiR) by gel-free capillary electrophoresis. I worked in the process of developing the second the generation DQAMmiR, which is simpler and more robust than the first generation, in regards, of omitting the addition of external agents (SSB) to separate the target-bound probes from the target-unbound probes, by the incorporation of electrically neutral polymer, PNAs, as hybridization probes. Yet, for separating the PNA–miRNA hybrids from each other we were still required to conjugate peptide drag tags on PNA probes. Our approach and logistics were confirmed by the proof-of-principle study: firstly, to see separation between the hybrid and excess probe using a single miRNA and secondly, using peptide drag to simultaneously quantify three different targets with appreciable accuracy and precision. Later, my study also involved the validation of our developed method in the prostate cancer-derived cell lysate to show good linearity, accuracy and precision, irrespective of sample matrix. In addition, our assay was able to detect endogenous PCa-upregulated miRNA without performing any extraction and/or miRNA amplification.

Our lab is currently working to take the assay to its next level of clinical validation to analyze cancer-deregulated miRNAs at lower LOD and LOQ in actual patient-derived samples (tissues and biofluids such as, urine, blood, *etc*) accurately, specifically and reproducibly.

REFERENCES

1. Strimbu, K. and J.A. Tavel, *What are biomarkers?* Current opinion in HIV and AIDS, 2010. **5**(6): p. 463-466.
2. Cagney, D.N., et al., *The FDA NIH Biomarkers, EndpointS, and other Tools (BEST) resource in neuro-oncology.* Neuro-Oncology, 2017. **20**(9): p. 1162-1172.
3. Poste, G., *Bring on the biomarkers.* Nature, 2011. **469**: p. 156.
4. Ray, P.M.D.P.D., et al., *Statistical Evaluation of a Biomarker.* Anesthesiology: The Journal of the American Society of Anesthesiologists, 2010. **112**(4): p. 1023-1040.
5. Drucker, E. and K. Krapfenbauer, *Pitfalls and limitations in translation from biomarker discovery to clinical utility in predictive and personalised medicine.* Epma j, 2013. **4**(1): p. 7.
6. Ausweger, C., et al., *Economic concerns about global healthcare in lung, head and neck cancer: meeting the economic challenge of predictive, preventive and personalized medicine.* The EPMA journal, 2010. **1**(4): p. 627-631.
7. Koehn, J. and K. Krapfenbauer, *Advanced proteomics procedure as a detection tool for predictive screening in type 2 pre-Diabetes.* The EPMA journal, 2010. **1**(1): p. 19-31.
8. Bushati, N. and S.M. Cohen, *microRNA Functions.* Annual Review of Cell and Developmental Biology, 2007. **23**(1): p. 175-205.
9. Stroynowska-Czerwinska, A., A. Fiszer, and W.J. Krzyzosiak, *The panorama of miRNA-mediated mechanisms in mammalian cells.* Cellular and molecular life sciences : CMLS, 2014. **71**(12): p. 2253-2270.
10. Lee, R.C., R.L. Feinbaum, and V. Ambros, *The C. elegans heterochronic gene lin-4 encodes small RNAs with antisense complementarity to lin-14.* Cell, 1993. **75**(5): p. 843-854.
11. He, L. and G.J. Hannon, *MicroRNAs: small RNAs with a big role in gene regulation.* Nature Reviews Genetics, 2004. **5**(7): p. 522-531.
12. Kim, V.N., J. Han, and M.C. Siomi, *Biogenesis of small RNAs in animals.* Nature Reviews Molecular Cell Biology, 2009. **10**: p. 126.
13. Khvorova, A., A. Reynolds, and S.D. Jayasena, *Functional siRNAs and miRNAs Exhibit Strand Bias.* Cell, 2003. **115**(2): p. 209-216.
14. de Planell-Saguer, M. and M.C. Rodicio, *Analytical aspects of microRNA in diagnostics: A review.* Analytica Chimica Acta, 2011. **699**(2): p. 134-152.
15. Lu, J., et al., *MicroRNA expression profiles classify human cancers.* Nature, 2005. **435**(7043): p. 834-838.
16. van Rooij, E., *The Art of MicroRNA Research.* Circulation Research, 2011. **108**(2): p. 219-234.
17. Cortez, M.A. and G.A. Calin, *MicroRNA identification in plasma and serum: a new tool to diagnose and monitor diseases.* Expert Opinion on Biological Therapy, 2009. **9**(6): p. 703-711.
18. Nelson, D.M., et al., *Advanced Techniques in Placental Biology—Workshop Report.* Placenta, 2006. **27**: p. 87-90.
19. Bovell, L., et al., *miRNAs are stable in colorectal cancer archival tissue blocks.* Frontiers in bioscience (Elite edition), 2012. **4**: p. 1937-1940.
20. Pathak, A.K., et al., *Circulating Cell-Free DNA in Plasma/Serum of Lung Cancer Patients as a Potential Screening and Prognostic Tool.* Clinical Chemistry, 2006. **52**(10): p. 1833.
21. Garzon, R., et al., *MicroRNA expression and function in cancer.* Trends in Molecular Medicine, 2006. **12**(12): p. 580-587.
22. Volinia, S., et al., *A microRNA expression signature of human solid tumors defines cancer gene targets.* Proceedings of the National Academy of Sciences, 2006. **103**(7): p. 2257.

23. Croce, C.M., *Oncogenes and Cancer.* New England Journal of Medicine, 2008. **358**(5): p. 502-511.
24. Choudhury, Y., et al., *Attenuated adenosine-to-inosine editing of microRNA-376a* promotes invasiveness of glioblastoma cells.* The Journal of clinical investigation, 2012. **122**(11): p. 4059-4076.
25. Stahlhut, C. and F.J. Slack, *MicroRNAs and the cancer phenotype: profiling, signatures and clinical implications.* Genome medicine, 2013. **5**(12): p. 111-111.
26. Válóczi, A., et al., *Sensitive and specific detection of microRNAs by northern blot analysis using LNA-modified oligonucleotide probes.* Nucleic Acids Research, 2004. **32**(22): p. e175-e175.
27. Castoldi, M., et al., *A sensitive array for microRNA expression profiling (miChip) based on locked nucleic acids (LNA).* RNA (New York, N.Y.), 2006. **12**(5): p. 913-920.
28. Chen, C., et al., *Real-time quantification of microRNAs by stem–loop RT–PCR.* Nucleic Acids Research, 2005. **33**(20): p. e179-e179.
29. Wang, H., R.A. Ach, and B. Curry, *Direct and sensitive miRNA profiling from low-input total RNA.* RNA (New York, N.Y.), 2007. **13**(1): p. 151-159.
30. Jiang, L., et al., *Direct microRNA detection with universal tagged probe and time-resolved fluorescence technology.* Biosensors and Bioelectronics, 2012. **34**(1): p. 291-295.
31. Husale, S., H.H.J. Persson, and O. Sahin, *DNA nanomechanics allows direct digital detection of complementary DNA and microRNA targets.* Nature, 2009. **462**: p. 1075.
32. Goo, N.-I. and D.-E. Kim, *Rolling circle amplification as isothermal gene amplification in molecular diagnostics.* BioChip Journal, 2016. **10**(4): p. 262-271.
33. Baskerville, S. and D.P. Bartel, *Microarray profiling of microRNAs reveals frequent coexpression with neighboring miRNAs and host genes.* RNA (New York, N.Y.), 2005. **11**(3): p. 241-247.
34. Shingara, J., et al., *An optimized isolation and labeling platform for accurate microRNA expression profiling.* RNA (New York, N.Y.), 2005. **11**(9): p. 1461-1470.
35. Varkonyi-Gasic, E. and R.P. Hellens, *Quantitative Stem-Loop RT-PCR for Detection of MicroRNAs*, in *RNAi and Plant Gene Function Analysis: Methods and Protocols*, H. Kodama and A. Komamine, Editors. 2011, Humana Press: Totowa, NJ. p. 145-157.
36. Kroh, E.M., et al., *Analysis of circulating microRNA biomarkers in plasma and serum using quantitative reverse transcription-PCR (qRT-PCR).* Methods (San Diego, Calif.), 2010. **50**(4): p. 298-301.
37. Debey-Pascher, S., et al., *Blood-Based miRNA Preparation for Noninvasive Biomarker Development*, in *Next-Generation MicroRNA Expression Profiling Technology: Methods and Protocols*, J.-B. Fan, Editor. 2012, Humana Press: Totowa, NJ. p. 307-338.
38. Zhao, B., et al., *A simple and fast method for profiling microRNA expression from low-input total RNA by microarray.* IUBMB Life, 2012. **64**(7): p. 612-616.
39. Wightman, B., I. Ha, and G. Ruvkun, *Posttranscriptional regulation of the heterochronic gene lin-14 by lin-4 mediates temporal pattern formation in C. elegans.* Cell, 1993. **75**(5): p. 855-862.
40. Wegman, D. and S. Krylov, *Direct miRNA-hybridization assays and their potential in diagnostics*. Vol. 44. 2013. 121–130.
41. Liu, C.-G., et al., *An oligonucleotide microchip for genome-wide microRNA profiling in human and mouse tissues.* Proceedings of the National Academy of Sciences of the United States of America, 2004. **101**(26): p. 9740-9744.
42. Wegman, D.W., et al., *Highly-Sensitive Amplification-Free Analysis of Multiple miRNAs by Capillary Electrophoresis.* Analytical Chemistry, 2015. **87**(2): p. 1404-1410.
43. Ban, E. and E.J. Song, *Recent developments and applications of capillary electrophoresis with laser-induced fluorescence detection in biological samples.* Journal of Chromatography B, 2013. **929**: p. 180-186.

44. Sempere, L.F., et al., *Expression profiling of mammalian microRNAs uncovers a subset of brain-expressed microRNAs with possible roles in murine and human neuronal differentiation.* Genome biology, 2004. **5**(3): p. R13-R13.
45. Válóczi, A., et al., *Sensitive and specific detection of microRNAs by northern blot analysis using LNA-modified oligonucleotide probes.* Nucleic acids research, 2004. **32**(22): p. e175-e175.
46. Várallyay, É., J. Burgyán, and Z. Havelda, *MicroRNA detection by northern blotting using locked nucleic acid probes.* Nature Protocols, 2008. **3**: p. 190.
47. Maroney, P.A., et al., *Direct detection of small RNAs using splinted ligation.* Nature Protocols, 2008. **3**: p. 279.
48. de Bang, T.C., et al., *Multiplexed microRNA Detection Using Lanthanide-Labeled DNA Probes and Laser Ablation Inductively Coupled Plasma Mass Spectrometry.* Analytical Chemistry, 2014. **86**(14): p. 6823-6826.
49. Liu, C.-G., et al., *MicroRNA expression profiling using microarrays.* Nature Protocols, 2008. **3**: p. 563.
50. Li, W. and K. Ruan, *MicroRNA detection by microarray.* Analytical and Bioanalytical Chemistry, 2009. **394**(4): p. 1117-1124.
51. Calin, G.A., et al., *MicroRNA profiling reveals distinct signatures in B cell chronic lymphocytic leukemias.* Proceedings of the National Academy of Sciences of the United States of America, 2004. **101**(32): p. 11755-11760.
52. Obernosterer, G., J. Martinez, and M. Alenius, *Locked nucleic acid-based in situ detection of microRNAs in mouse tissue sections.* Nature Protocols, 2007. **2**: p. 1508.
53. Nelson, P.T., et al., *RAKE and LNA-ISH reveal microRNA expression and localization in archival human brain.* RNA (New York, N.Y.), 2006. **12**(2): p. 187-191.
54. Deo, M., et al., *Detection of mammalian microRNA expression by in situ hybridization with RNA oligonucleotides.* Developmental Dynamics, 2006. **235**(9): p. 2538-2548.
55. de Planell-Saguer, M., M.C. Rodicio, and Z. Mourelatos, *Rapid in situ codetection of noncoding RNAs and proteins in cells and formalin-fixed paraffin-embedded tissue sections without protease treatment.* Nature Protocols, 2010. **5**: p. 1061.
56. Nuovo, G., et al., *In situ detection of mature microRNAs by labeled extension on ultramer templates.* BioTechniques, 2009. **46**(2): p. 115-126.
57. Nuovo, G., et al., *Nuovo GJ, Elton TS, Nana-Sinkam P, Volinia S, Croce CM, Schmittgen TD.. A methodology for the combined in situ analyses of the precursor and mature forms of microRNAs and correlation with their putative targets. Nat Protoc 4: 107-115*. Vol. 4. 2009. 107-15.
58. Neely, L.A., et al., *A single-molecule method for the quantitation of microRNA gene expression.* Nature Methods, 2005. **3**: p. 41.
59. Li, D., et al., *xMAP Array Microspheres Based Stem–Loop Structured Probes as Conformational Switches for Multiplexing Detection of miRNAs.* Analytical Chemistry, 2014. **86**(20): p. 10148-10156.
60. Lee, H., et al., *Encoded Hydrogel Microparticles for Sensitive and Multiplex microRNA Detection Directly from Raw Cell Lysates.* Analytical Chemistry, 2016. **88**(6): p. 3075-3081.
61. Zhou, W., et al., *Simultaneous Surface-Enhanced Raman Spectroscopy Detection of Multiplexed MicroRNA Biomarkers.* Analytical Chemistry, 2017. **89**(11): p. 6120-6128.
62. Ryoo, S.-R., et al., *Quantitative and Multiplexed MicroRNA Sensing in Living Cells Based on Peptide Nucleic Acid and Nano Graphene Oxide (PANGO).* ACS Nano, 2013. **7**(7): p. 5882-5891.
63. Esteban-Fernández de Ávila, B., et al., *Single Cell Real-Time miRNAs Sensing Based on Nanomotors.* ACS Nano, 2015. **9**(7): p. 6756-6764.
64. Zhou, X., et al., *Phage-mediated counting by the naked eye of miRNA molecules at attomolar concentrations in a Petri dish.* Nature materials, 2015. **14**(10): p. 1058-1064.

65. Zheng, X., et al., *Label-free detection of microRNA based on coupling multiple isothermal amplification techniques.* Scientific reports, 2016. **6**: p. 35982-35982.
66. Ro, S., et al., *A PCR-based method for detection and quantification of small RNAs.* Biochemical and biophysical research communications, 2006. **351**(3): p. 756-763.
67. Takada, S. and H. Mano, *Profiling of microRNA expression by mRAP.* Nature Protocols, 2007. **2**: p. 3136.
68. Cui, L., et al., *Graphene oxide-protected DNA probes for multiplex microRNA analysis in complex biological samples based on a cyclic enzymatic amplification method.* Chemical Communications, 2012. **48**(2): p. 194-196.
69. Xie, Y., et al., *Highly sensitive and selective detection of miRNA: DNase I-assisted target recycling using DNA probes protected by polydopamine nanospheres.* Chemical Communications, 2015. **51**(11): p. 2156-2158.
70. Zhu, W., et al., *A label-free and PCR-free electrochemical assay for multiplexed microRNA profiles by ligase chain reaction coupling with quantum dots barcodes.* Biosensors and Bioelectronics, 2014. **53**: p. 414-419.
71. Yuan, Z., et al., *Homogeneous and Sensitive Detection of microRNA with Ligase Chain Reaction and Lambda Exonuclease-Assisted Cationic Conjugated Polymer Biosensing.* ACS Applied Materials & Interfaces, 2014. **6**(9): p. 6181-6185.
72. Ge, J., et al., *A Highly Sensitive Target-Primed Rolling Circle Amplification (TPRCA) Method for Fluorescent in Situ Hybridization Detection of MicroRNA in Tumor Cells.* Analytical Chemistry, 2014. **86**(3): p. 1808-1815.
73. Van Ness, J., L.K. Van Ness, and D.J. Galas, *Isothermal reactions for the amplification of oligonucleotides.* Proceedings of the National Academy of Sciences of the United States of America, 2003. **100**(8): p. 4504-4509.
74. Gao, Z. and Z. Yang, *Detection of MicroRNAs Using Electrocatalytic Nanoparticle Tags.* Analytical Chemistry, 2006. **78**(5): p. 1470-1477.
75. Wark, A.W., H.J. Lee, and R.M. Corn, *Multiplexed detection methods for profiling microRNA expression in biological samples.* Angewandte Chemie (International ed. in English), 2008. **47**(4): p. 644-652.
76. Garibyan, L. and N. Avashia, *Polymerase chain reaction.* The Journal of investigative dermatology, 2013. **133**(3): p. 1-4.
77. Cissell, K.A., S. Campbell, and S.K. Deo, *Rapid, single-step nucleic acid detection.* Analytical and Bioanalytical Chemistry, 2008. **391**(7): p. 2577.
78. Cissell, K.A., et al., *Reassembly of a Bioluminescent Protein Renilla Luciferase Directed through DNA Hybridization.* Bioconjugate Chemistry, 2009. **20**(1): p. 15-19.
79. Zhang, G.-J., et al., *Label-free direct detection of MiRNAs with silicon nanowire biosensors.* Biosensors and Bioelectronics, 2009. **24**(8): p. 2504-2508.
80. Fan, Y., et al., *Detection of MicroRNAs Using Target-Guided Formation of Conducting Polymer Nanowires in Nanogaps.* Journal of the American Chemical Society, 2007. **129**(17): p. 5437-5443.
81. Gao, Z. and Y.H. Yu, *Direct labeling microRNA with an electrocatalytic moiety and its application in ultrasensitive microRNA assays.* Biosensors and Bioelectronics, 2007. **22**(6): p. 933-940.
82. Gao, Z. and Y.H. Yu, *A microRNA biosensor based on direct chemical ligation and electrochemically amplified detection.* Sensors and Actuators B: Chemical, 2007. **121**(2): p. 552-559.
83. Labib, M., et al., *Three-Mode Electrochemical Sensing of Ultralow MicroRNA Levels.* Journal of the American Chemical Society, 2013. **135**(8): p. 3027-3038.
84. Linsen, S.E.V., et al., *Limitations and possibilities of small RNA digital gene expression profiling.* Nature Methods, 2009. **6**: p. 474.

85. Weng, L., et al., *MicroRNA profiling of clear cell renal cell carcinoma by whole-genome small RNA deep sequencing of paired frozen and formalin-fixed, paraffin-embedded tissue specimens.* The Journal of Pathology, 2010. **222**(1): p. 41-51.
86. Shamsi, M., et al., *Electrochemiluminescence on digital microfluidics for microRNA analysis*. 2015.
87. Gao, X., et al., *Visual detection of microRNA with lateral flow nucleic acid biosensor.* Biosensors & bioelectronics, 2014. **54**: p. 578-584.
88. Deng, H., et al., *Quantum dots-labeled strip biosensor for rapid and sensitive detection of microRNA based on target-recycled nonenzymatic amplification strategy*. Biosensors and Bioelectronics, 2017. **87**: p. 931-940.
89. Deng, H., et al., *Paperfluidic Chip Device for Small RNA Extraction, Amplification, and Multiplexed Analysis.* ACS Applied Materials & Interfaces, 2017. **9**(47): p. 41151-41158.
90. Qavi, A.J. and R.C. Bailey, *Multiplexed detection and label-free quantitation of microRNAs using arrays of silicon photonic microring resonators.* Angewandte Chemie (International ed. in English), 2010. **49**(27): p. 4608-4611.
91. Gordon, J.E.A., et al., *Validation of nanostring microrna analysis in leukaemic blood.* Pathology, 2014. **46**: p. S93.
92. Tedeschi, T., et al., *Detection of the R553X DNA single point mutation related to cystic fibrosis by a "chiral box" D-lysine-peptide nucleic acid probe by capillary electrophoresis.* ELECTROPHORESIS, 2005. **26**(22): p. 4310-4316.
93. Tsukada, H., et al., *Quantitative single-nucleotide polymorphism analysis in secondary-structured DNA by affinity capillary electrophoresis using a polyethylene glycol–peptide nucleic acid block copolymer.* Analytical Biochemistry, 2013. **433**(2): p. 150-152.
94. Park, S.H., et al., *Capillary electrophoretic mobility shift assay for binding of DNA with NFAT3, a transcription factor from H9c2 cardiac myoblast cells.* ELECTROPHORESIS, 2011. **32**(16): p. 2174-2180.
95. Ahmad Khan, H., *Detection and semi-quantitative determination of low abundance GFAP mRNA in mouse brain by capillary electrophoresis coupled with laser-induced fluorescence.* Brain Research Protocols, 2004. **14**(1): p. 13-17.
96. Li, N., et al., *Separation of miRNA and its methylation products by capillary electrophoresis.* Journal of chromatography. A, 2008. **1202**(2): p. 220-223.
97. Chang, P.-L., et al., *Analysis of BART7 MicroRNA from Epstein−Barr Virus-Infected Nasopharyngeal Carcinoma Cells by Capillary Electrophoresis.* Analytical Chemistry, 2008. **80**(22): p. 8554-8560.
98. Schoch, R.B., M. Ronaghi, and J.G. Santiago, *Rapid and selective extraction, isolation, preconcentration, and quantitation of small RNAs from cell lysate using on-chip isotachophoresis.* Lab on a Chip, 2009. **9**(15): p. 2145-2152.
99. Ban, E. and E.J. Song, *Capillary electrophoresis methods for microRNAs assays: A review.* Analytica Chimica Acta, 2014. **852**: p. 1-7.
100. Ban, E., D.-K. Chae, and E.J. Song, *Determination of micro-RNA in cardiomyoblast cells using CE with LIF detection.* ELECTROPHORESIS, 2013. **34**(4): p. 598-604.
101. Garcia-Schwarz, G. and J.G. Santiago, *Integration of On-Chip Isotachophoresis and Functionalized Hydrogels for Enhanced-Sensitivity Nucleic Acid Detection.* Analytical Chemistry, 2012. **84**(15): p. 6366-6369.
102. Kovacs-Nagy, R., et al., *Haplotyping of putative microRNA-binding sites in the SNAP-25 gene.* ELECTROPHORESIS, 2011. **32**(15): p. 2013-2020.
103. Rahman, O.A., et al., *Analysis of a polymorphic microRNA target site in the purinergic receptor P2RX7 gene.* ELECTROPHORESIS, 2010. **31**(11): p. 1790-1795.

104. Khan, N., et al., *Quantitative Analysis of MicroRNA in Blood Serum with Protein-Facilitated Affinity Capillary Electrophoresis.* Analytical Chemistry, 2011. **83**(16): p. 6196-6201.
105. Khan, N., G. Mironov, and M.V. Berezovski, *Direct detection of endogenous MicroRNAs and their post-transcriptional modifications in cancer serum by capillary electrophoresis-mass spectrometry.* Analytical and Bioanalytical Chemistry, 2016. **408**(11): p. 2891-2899.
106. Williams, G., et al., *Characterisation of body fluid specific microRNA markers by capillary electrophoresis.* Forensic Science International: Genetics Supplement Series, 2013. **4**(1): p. e274-e275.
107. Wegman, D.W., et al., *Achieving Single-Nucleotide Specificity in Direct Quantitative Analysis of Multiple MicroRNAs (DQAMmiR).* Analytical Chemistry, 2016. **88**(4): p. 2472-2477.
108. Ghasemi, F., et al., *Improvements to direct quantitative analysis of multiple microRNAs facilitating faster analysis.* Analytical chemistry, 2013. **85**(21): p. 10062-10066.
109. Mazouchi, A., et al., *Ultrasensitive on-column laser-induced fluorescence in capillary electrophoresis using multiparameter confocal detection.* Analyst, 2012. **137**(23): p. 5538-5545.
110. Dodgson, B.J., et al., *Detection of a Thousand Copies of miRNA without Enrichment or Modification.* Analytical Chemistry, 2012. **84**(13): p. 5470-5474.
111. Wegman, D.W. and S.N. Krylov, *Direct Quantitative Analysis of Multiple miRNAs (DQAMmiR).* Angewandte Chemie International Edition, 2011. **50**(44): p. 10335-10339.
112. Krylova, S.M., D.W. Wegman, and S.N. Krylov, *Making DNA hybridization assays in capillary electrophoresis quantitative.* Analytical chemistry, 2010. **82**(11): p. 4428-4433.
113. Wegman, D.W., et al., *Universal Drag Tag for Direct Quantitative Analysis of Multiple MicroRNAs.* Analytical Chemistry, 2013. **85**(13): p. 6518-6523.
114. Nielsen, P. and M. Egholm, *An Introduction to Peptide Nucleic Acid*. Vol. 1. 1999. 89-104.
115. Nielsen, P., et al., *Sequence-Selective Recognition of DNA by Strand Displacement with a Thymine-Substituted Polyamide*. Vol. 254. 1992. 1497-500.
116. Hyrup, B. and P.E. Nielsen, *Peptide Nucleic Acids (PNA): Synthesis, properties and potential applications.* Bioorganic & Medicinal Chemistry, 1996. **4**(1): p. 5-23.
117. Avitabile, C., et al., *Development of an efficient and low-cost protocol for the manual PNA synthesis by Fmoc chemistry.* Tetrahedron Letters, 2010. **51**(29): p. 3716-3718.
118. Lee, H., et al., *Peptide Nucleic Acid Synthesis by Novel Amide Formation.* Organic Letters, 2007. **9**(17): p. 3291-3293.
119. Park, H., et al., *Effect of ionic strength on PNA-DNA hybridization on surfaces and in solution.* Biointerphases, 2007. **2**(2): p. 80-88.
120. Perry-O'Keefe, H., et al., *Peptide nucleic acid pre-gel hybridization: an alternative to southern hybridization.* Proceedings of the National Academy of Sciences of the United States of America, 1996. **93**(25): p. 14670-14675.
121. Basile, A., et al., *Use of peptide nucleic acid probes for detecting DNA single-base mutations by capillary electrophoresis.* ELECTROPHORESIS, 2002. **23**(6): p. 926-929.
122. Wang, X., et al., *Multiple modes of capillary electrophoresis applied in peptide nucleic acid related study.* Journal of Chromatography A, 2017. **1501**: p. 161-166.
123. Ostromohov, N., O. Schwartz, and M. Bercovici, *Focused upon Hybridization: Rapid and High Sensitivity Detection of DNA Using Isotachophoresis and Peptide Nucleic Acid Probes.* Analytical Chemistry, 2015. **87**(18): p. 9459-9466.
124. Metcalf, G.A.D., et al., *Amplification-Free Detection of Circulating microRNA Biomarkers from Body Fluids Based on Fluorogenic Oligonucleotide-Templated Reaction between Engineered Peptide Nucleic Acid Probes: Application to Prostate Cancer Diagnosis.* Analytical Chemistry, 2016. **88**(16): p. 8091-8098.

125. Kim, H., et al., *A PNA microarray platform for miRNA expression profiling using on-chip labeling technology.* BioChip Journal, 2012. **6**(1): p. 25-33.
126. Nagai, Y., et al., *Genetic Heterogeneity of the Epidermal Growth Factor Receptor in Non–Small Cell Lung Cancer Cell Lines Revealed by a Rapid and Sensitive Detection System, the Peptide Nucleic Acid-Locked Nucleic Acid PCR Clamp.* Cancer Research, 2005. **65**(16): p. 7276.
127. Sahu, B., et al., *Synthesis and characterization of conformationally preorganized, (R)-diethylene glycol-containing γ-peptide nucleic acids with superior hybridization properties and water solubility.* The Journal of organic chemistry, 2011. **76**(14): p. 5614-5627.
128. Zanardi, C., et al., *Peptide nucleic acids tagged with four lysine residues for amperometric genosensors.* Artificial DNA, PNA & XNA, 2012. **3**(2): p. 80-87.
129. Koppelhus, U. and P.E. Nielsen, *Cellular delivery of peptide nucleic acid (PNA).* Advanced Drug Delivery Reviews, 2003. **55**(2): p. 267-280.
130. Bonora, G.M., et al., *PNA Conjugated to High-Molecular Weight Poly(Ethylene Glycol): Synthesis and Properties.* Nucleosides, Nucleotides and Nucleic Acids, 2007. **26**(6-7): p. 661-664.
131. Colin, H., et al., *The role of the temperature in reversed-phase high-performance liquid chromatography using pyrocarbon-containing adsorbents.* Journal of Chromatography A, 1978. **167**: p. 41-65.
132. Kiliszek, A., et al., *The first crystal structures of RNA-PNA duplexes and a PNA-PNA duplex containing mismatches--toward anti-sense therapy against TREDs.* Nucleic acids research, 2016. **44**(4): p. 1937-1943.
133. Zhan, Y. and G. Zocchi, *Flexibility of DNA/PNA, DNA/LNA, DNA/RNA hybrids measured with a nanoscale transducer.* EPL (Europhysics Letters), 2017. **119**(4): p. 48005.
134. Brinkers, S., et al., *The persistence length of double stranded DNA determined using dark field tethered particle motion.* The Journal of Chemical Physics, 2009. **130**(21): p. 215105.
135. Happel, J. and H. Brenner, *The Motion of a Rigid Particle of Arbitrary Shape in an Unbounded Fluid*, in *Low Reynolds number hydrodynamics: with special applications to particulate media*, J. Happel and H. Brenner, Editors. 1983, Springer Netherlands: Dordrecht. p. 159-234.
136. Gagliardi, L.G., et al., *δ Conversion Parameter between pH Scales (and) in Acetonitrile/Water Mixtures at Various Compositions and Temperatures.* Analytical Chemistry, 2007. **79**(8): p. 3180-3187.
137. Wilkins, D.K., et al., *Hydrodynamic Radii of Native and Denatured Proteins Measured by Pulse Field Gradient NMR Techniques.* Biochemistry, 1999. **38**(50): p. 16424-16431.
138. Kaneta, T., S. Tanaka, and H. Yoshida, *Improvement of resolution in the capillary electrophoretic separation of catecholamines by complex formation with boric acid and control of electroosmosis with a cationic surfactant.* Journal of Chromatography A, 1991. **538**(2): p. 385-391.
139. Nakayama, H., et al., *Direct Identification of Human Cellular MicroRNAs by Nanoflow Liquid Chromatography–High-Resolution Tandem Mass Spectrometry and Database Searching.* Analytical Chemistry, 2015. **87**(5): p. 2884-2891.
140. Yang, C., et al., *Multiplexed and Amplified Electronic Sensor for the Detection of MicroRNAs from Cancer Cells.* Analytical Chemistry, 2014. **86**(23): p. 11913-11918.
141. Shen, M.M. and C. Abate-Shen, *Molecular genetics of prostate cancer: new prospects for old challenges.* Genes & development, 2010. **24**(18): p. 1967-2000.
142. Pauler Ankerst, D. and I. M Thompson, *Sensitivity and specificity of prostate-specific antigen for prostate cancer detection with high rates of biopsy verification*. Vol. 78. 2006. 125-9.
143. Luu, H.N., et al., *miRNAs associated with prostate cancer risk and progression.* BMC urology, 2017. **17**(1): p. 18-18.

144. Guo, J., et al., *miR-20b promotes cellular proliferation and migration by directly regulating phosphatase and tensin homolog in prostate cancer.* Oncology letters, 2017. **14**(6): p. 6895-6900.
145. Wang, M., et al., *Loss of miR-100 enhances migration, invasion, epithelial-mesenchymal transition and stemness properties in prostate cancer cells through targeting Argonaute 2*. Vol. 45. 2014.
146. Brown, R.B. and J. Audet, *Current techniques for single-cell lysis.* Journal of the Royal Society, Interface, 2008. **5 Suppl 2**(Suppl 2): p. S131-S138.
147. Turner, J.J., et al., *Cell-penetrating peptide conjugates of peptide nucleic acids (PNA) as inhibitors of HIV-1 Tat-dependent trans-activation in cells.* Nucleic acids research, 2005. **33**(21): p. 6837-6849.